



# mTORC1-independent translation control in mammalian cells by methionine adenosyltransferase 2A and S-adenosylmethionine

Received for publication, October 28, 2021, and in revised form, May 19, 2022. Published, Papers in Press, May 27, 2022.

<https://doi.org/10.1016/j.jbc.2022.102084>

Mahabub Alam<sup>1,2</sup>, Hiroki Shima<sup>1</sup>, Yoshitaka Matsuo<sup>3</sup>, Nguyen Chi Long<sup>1</sup>, Mitsuyo Matsumoto<sup>1</sup>, Yusho Ishii<sup>1</sup>, Nichika Sato<sup>3</sup>, Takato Sugiyama<sup>4</sup>, Risa Nobuta<sup>4</sup>, Satoshi Hashimoto<sup>4</sup>, Liang Liu<sup>1</sup>, Mika K. Kaneko<sup>5</sup>, Yukinari Kato<sup>5,6</sup>, Toshifumi Inada<sup>3,\*</sup>, and Kazuhiko Igarashi<sup>1,\*</sup>

From the <sup>1</sup>Department of Biochemistry, Tohoku University Graduate School of Medicine, Sendai, Japan; <sup>2</sup>Department of Animal Science and Nutrition, Faculty of Veterinary Medicine, Chattogram Veterinary and Animal Sciences University, Chattogram, Bangladesh; <sup>3</sup>Division of RNA and Gene Regulation, Institute of Medical Science, The University of Tokyo, Tokyo, Japan; <sup>4</sup>Laboratory of Gene Regulation, Department of Molecular Biopharmacy and Genetics, <sup>5</sup>Department of Antibody Drug Development, and <sup>6</sup>Department of Molecular Pharmacology, Tohoku University Graduate School of Medicine, Sendai, Japan

Edited by Karin Musier-Forsyth

Methionine adenosyltransferase (MAT) catalyzes the synthesis of S-adenosylmethionine (SAM). As the sole methyl-donor for methylation of DNA, RNA, and proteins, SAM levels affect gene expression by changing methylation patterns. Expression of MAT2A, the catalytic subunit of isozyme MAT2, is positively correlated with proliferation of cancer cells; however, how MAT2A promotes cell proliferation is largely unknown. Given that the protein synthesis is induced in proliferating cells and that RNA and protein components of translation machinery are methylated, we tested here whether MAT2 and SAM are coupled with protein synthesis. By measuring ongoing protein translation *via* puromycin labeling, we revealed that MAT2A depletion or chemical inhibition reduced protein synthesis in HeLa and Hepa1 cells. Furthermore, overexpression of MAT2A enhanced protein synthesis, indicating that SAM is limiting under normal culture conditions. In addition, MAT2 inhibition did not accompany reduction in mechanistic target of rapamycin complex 1 activity but nevertheless reduced polysome formation. Polysome-bound RNA sequencing revealed that MAT2 inhibition decreased translation efficiency of some fraction of mRNAs. MAT2A was also found to interact with the proteins involved in rRNA processing and ribosome biogenesis; depletion or inhibition of MAT2 reduced 18S rRNA processing. Finally, quantitative mass spectrometry revealed that some translation factors were dynamically methylated in response to the activity of MAT2A. These observations suggest that cells possess an mTOR-independent regulatory mechanism that tunes translation in response to the levels of SAM. Such a system may acclimate cells for survival when SAM synthesis is reduced, whereas it may support proliferation when SAM is sufficient.

Translation is the single largest energy expenditure sector of cellular metabolism which uses around 20% of the total energy of cells (1–3). Since aberrant translation leads to dissipation of energy resources and various pathological consequences, translation is tightly regulated by multiple signaling pathways in cells (4). Growth and proliferation of mammalian cells require signal-mediated stimulations of translation initiated by the availability of extracellular factors such as insulin and other growth factors, nutrition, endocrine secretions and metabolites. The proliferating cells integrate the presence of these extracellular molecules to induce translation (5, 6). So far as explored, the phosphoinositide 3-kinase–AKT and the mitogen-activated protein kinase pathways are the main upstream controllers of translation in cells (7, 8). Both pathways converge on mechanistic target of rapamycin complex 1 (mTORC1) to regulate translation. mTORC1 phosphorylates the inhibitory eukaryotic translation initiation factor 4E binding proteins (4E-BP1 and 2) to detach them from eukaryotic translation initiation factor 4E. The released eukaryotic translation initiation factor 4E then aids the formation of the translation initiation complex at the 5' ends of mRNA, thereby enhancing global translation (9). Besides the global translation stimulation, mTORC1 also boosts translation of mRNA bearing the 5' terminal oligopyrimidine tract (10). Moreover, mTORC1 phosphorylates ribosomal protein p70 S6 kinase (S6K) that is required for the positive regulation of eukaryotic initiation factor 4A (eIF4A) and 4B (eIF4B) to augment translation (11–14).

Cancer cells acquire the ability to induce protein synthesis, growth, and proliferation by activating the translation signaling pathways which facilitate the expression of proteins required for cell survival and growth (15–17). In addition, translation induction can be caused by alteration of expression and/or phosphorylation of diverse proteins involved in translation. For example, consecutive expression and phosphorylation of eukaryotic initiation factor 4F accelerated translation initiation (15, 18–20). Reduced expression or increased

\* For correspondence: Kazuhiko Igarashi, [igarashi@med.tohoku.ac.jp](mailto:igarashi@med.tohoku.ac.jp); Toshifumi Inada, [toshiinada@ims.u-tokyo.ac.jp](mailto:toshiinada@ims.u-tokyo.ac.jp).

## ***mTORC1-independent translation control by MAT2A and SAM***

phosphorylation of 4E-BPs promoted translation in pancreatic cancer (21). Overexpression of eukaryotic initiation factor 3 induced global protein synthesis and increased translation of oncogenic transcripts in immortalized fibroblastic cells (22). Due to the contribution of mTOR to translation, cellular growth, and proliferation, various drugs targeting the mTOR pathway are being developed for cancer therapy (23–25). However, one of the major problems of mTOR inhibition for cancer therapy is that upon inhibition of a protein in the mTOR signaling, cancer cells develop a resistance to the chemotherapy by activating compensatory proteins by various feedback mechanisms (26). For example, upon inhibition of mTORC1, the AKT and mitogen-activated protein kinase pathways are activated by feedback mechanisms to promote cell survival (27–31). Therefore, it is of utmost importance to explore new mTOR-independent translation regulatory mechanisms to propose novel targets for cancer therapy.

The one-carbon metabolic cycle of methionine is intimately connected with the mTOR signaling (32). It is known that the mTOR signaling is responsive to *S*-adenosylmethionine (SAM), one of the one-carbon cycle metabolites, owing to the SAMTOR protein acting as the SAM-sensor (33). SAM is produced from methionine and ATP by methionine adenosyltransferase (MAT). In mammals, three isozymes of MAT are known (34, 35). MAT1 and MAT3 are found in liver, whereas MAT2 is expressed in all tissues except for adult liver (36–38). MAT2 consists of two subunits: MAT2A and MAT2B, which form a complex with a molecular ratio of 2:1. MAT2A is the catalytic subunit, whereas MAT2B has been suggested to regulate the catalytic activity (39) or stability (40) of MAT2A. MAT2A is expressed in proliferating fetal hepatocytes and is replaced by MAT1 in adult quiescent hepatocytes (41). Upon partial hepatectomy, MAT2A is upregulated during regeneration (42). Also, the expression of MAT2A is known to be high in various cancers including those of liver (43, 44), uterine cervix (45), colon (46), and breast (47). These observations suggest that MAT2A is required for cell growth and proliferation. Recently, MYC has been shown to induce MAT2A expression (48), which explains how MAT2A is upregulated in proliferative tissue and particularly in cancer. These pieces of evidence suggest that SAM synthesis by MAT2A is connected to cancer cell growth and proliferation. However, whether the connection is mediated exclusively by the mTOR pathway remains unknown.

SAM is the essential methyl group donor in biological methylation of various biomolecules. Methylation in DNA, RNA, and histone proteins is well-studied due to its critical roles in gene expression control. Besides histones, non-histone proteins such as ribosomal proteins and translation factors are also methylated (49). Although the biological significance of methylation in ribosomal proteins is yet to be interrogated, methylation of several translation factors is known to regulate translation. For example, depletion of the methyltransferase for lysine 165 of eEF1A (eEF1A165K) induced translation of proteins related to ribosome biogenesis and chromatin. In contrast, it reduced translation of proteins

important for unfolded protein response (50). Methylation of lysine 55 of eEF1A (eEF1A55K) promoted global translation in a human lung cancer cell line (51). As some of the protein components of translation machinery are methylated, we hypothesized that MAT2 and SAM are coupled with protein synthesis in mammalian cells by affecting their methylation. In this study, we discovered that MAT2A promotes protein synthesis in an mTORC1-independent manner. Polysome profiling and RNA sequencing revealed that MAT2A is required for the formation of active polysome and maintenance of translation efficiencies of mRNAs. Moreover, we found that MAT2A interacts with ribosome biogenesis factors and contributes to processing of the 18S rRNA and dynamic methylation of translation factors.

### **Results**

#### ***MAT2A is essential for global protein synthesis in the mammalian cells***

To reveal the involvement of MAT2A in protein synthesis, we examined the global protein synthesis rate upon *Mat2a* knockdown in the mouse hepatocellular carcinoma cell line (Hepa1) by using surface sensing of translation (SUnSET) (52). Elongating peptides in cultured cells were labeled for 30 min with the aminoglycoside antibiotic puromycin. Translation elongation is inhibited when translating ribosome incorporates puromycin into nascent proteins. The resulting short peptides labeled with puromycin can be detected by Western blotting using an antipuromycin antibody, which enables examination of the translation rate. We found that the global translation was reduced in Hepa1 cells in which MAT2A was depleted by siRNA (Figs. 1A and S1A). Treatment of cells with the translation inhibitor cycloheximide (CHX) greatly diminished the puromycin-labeled proteins, indicating that puromycin specifically labeled the nascent peptides (Fig. 1A: Lanes 5 and 6). In line with knockdown of *Mat2a*, chemical inhibition of MAT2A by cycloleucine (cLEU), which is a substrate-competitive inhibitor of MAT2 (53, 54), significantly reduced protein synthesis in HeLa cells (Fig. 1B). Note that the reduction in protein synthesis occurred within 1 h after the MAT2A inhibition (Fig. S1B). Next, we examined the effect of MAT2A overexpression on protein synthesis. We established HeLa cells stably expressing FLAG-Bio-tagged MAT2A (FB-MAT2A) (Fig. S1C). The FB-MAT2A protein was considered as functional as the native MAT2A protein since immunofluorescence microscopy using an anti-FLAG antibody confirmed that the FB-MAT2A was localized in nucleus as expected (Fig. S1D), and streptavidin affinity purification of FB-MAT2A showed its interaction with the endogenous MAT2B protein (Fig. S1E). By single-cell colony isolation of these cells, a high FB-MAT2A-expressing clone was selected for the following experiment. The FB-MAT2A-expressing cells cultured under a normal condition showed higher protein synthesis compared to the control cells established using the empty vector (FB-EV), indicating that MAT2A promoted protein synthesis (Fig. 1C).



## mTORC1-independent translation control by MAT2A and SAM

cells but not in the control cells (Fig. 1C, lanes 5–10). Importantly, the effect of FB-MAT2A was not diminished by the treatment with rapamycin. These results indicate that MAT2A does not rely on the mTORC1 activity to promote protein synthesis. mTORC1 is activated by various stimuli including growth factors and nutrients such as amino acids, exerting effects on translation machinery (Fig. S2). To further investigate whether MAT2A affects the mTOR signaling pathway, we examined the activation status of mTORC1 upon MAT2A perturbations. S6K is the downstream target of mTORC1. Since the amount of phosphorylated S6K (Phos-S6K) directly reflects the activity of the mTORC1 signaling (55), we examined the amount of Phos-S6K by Western blotting. The FB-MAT2A-expressing cells did not show any appreciable alteration in Phos-S6K compared to the control cells under the normal conditions or when the cells were starved and were restimulated with serum (Fig. 1C). Phos-S6K was unchanged upon MAT2A inhibition by cLEU in both HeLa (Fig. 2A) and Hepa1 (Fig. 2B) cells, whereas it was reduced in response to rapamycin. These results suggest that the effect of MAT2A on protein synthesis is not contingent on the activity of mTORC1.

### MAT2A and SAM are essential for maintaining active translation in cells

To elucidate the characteristics of the MAT2A-regulated protein synthesis, we carried out a polysome profiling of HeLa cells upon MAT2A inhibition by cLEU. Heavy polysome (also called active polysome) formation was impaired upon MAT2A inhibition with a concomitant increase of monosome (80S) and its subunits (40S and 60S) (Fig. 3A). These characteristics of polysome profile suggest that translation initiation to form monosomes was hampered, and only a smaller fraction

of successfully formed monosomes proceeded to active polysome formation.

To investigate the MAT2A-regulated translational control, we isolated translating mRNA from the polysome fractions and performed RNA sequencing. We found that after MAT2A inhibition, 507 transcripts were upregulated, and 193 were downregulated in the polysome occupancy (Fig. 3B and Table S1). The translation efficiency (TE) of each mRNA was calculated by a ratio of reads number between polysome fraction and total RNA, which showed that the number of transcripts with decreased TE (135) by MAT2A inhibition was greater than that of transcripts with increased TE (120) (Fig. 3C and Table S1). Next, we performed RNA-sequencing of the cells treated with or without cLEU. A total of 1147 and 328 transcripts, respectively, were upregulated and downregulated significantly ( $q < 0.01$ ) in total RNA fractions after MAT2A inhibition (Fig. 3D and Table S1). Gene ontology (GO) analysis revealed that the expression of genes involved in ribosome biogenesis was reduced in the cLEU-treated cells (Fig. 3E). These results strongly suggested the existence of a translation regulation mechanism involving MAT2A and SAM, which concerns the expression of a specific subset of mRNA through the altered formation of polysome.

### MAT2A interacts with proteins involved in ribosome biogenesis and translation

To understand the mechanism of the regulation of protein synthesis by MAT2A, we aimed to elucidate the MAT2A-interacting protein network. We purified FB-MAT2A from HeLa cells stably expressing FB-MAT2A by affinity purification with streptavidin. The purified proteins were then separated by sodium dodecyl sulphate-polyacrylamide gel electrophoresis (SDS-PAGE), were in-gel trypsin-digested, and

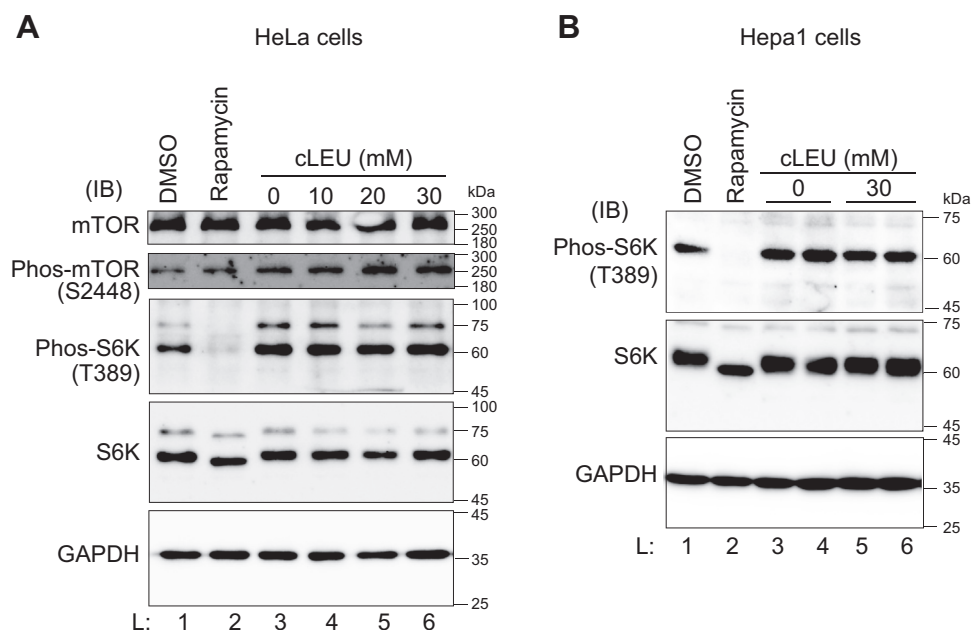


**Figure 2. MAT2A-regulated protein synthesis is independent of mTORC1.** A and B, Western blotting for the mTOR pathway proteins after treating cells at different concentrations of cLEU for 6 h using HeLa (A) and Hepa1 (B) cells. In lane 2, cells were treated with 400 nM rapamycin for 1 h. cLEU, cycloleucine; mTORC1, mechanistic target of rapamycin complex 1.

## mTORC1-independent translation control by MAT2A and SAM

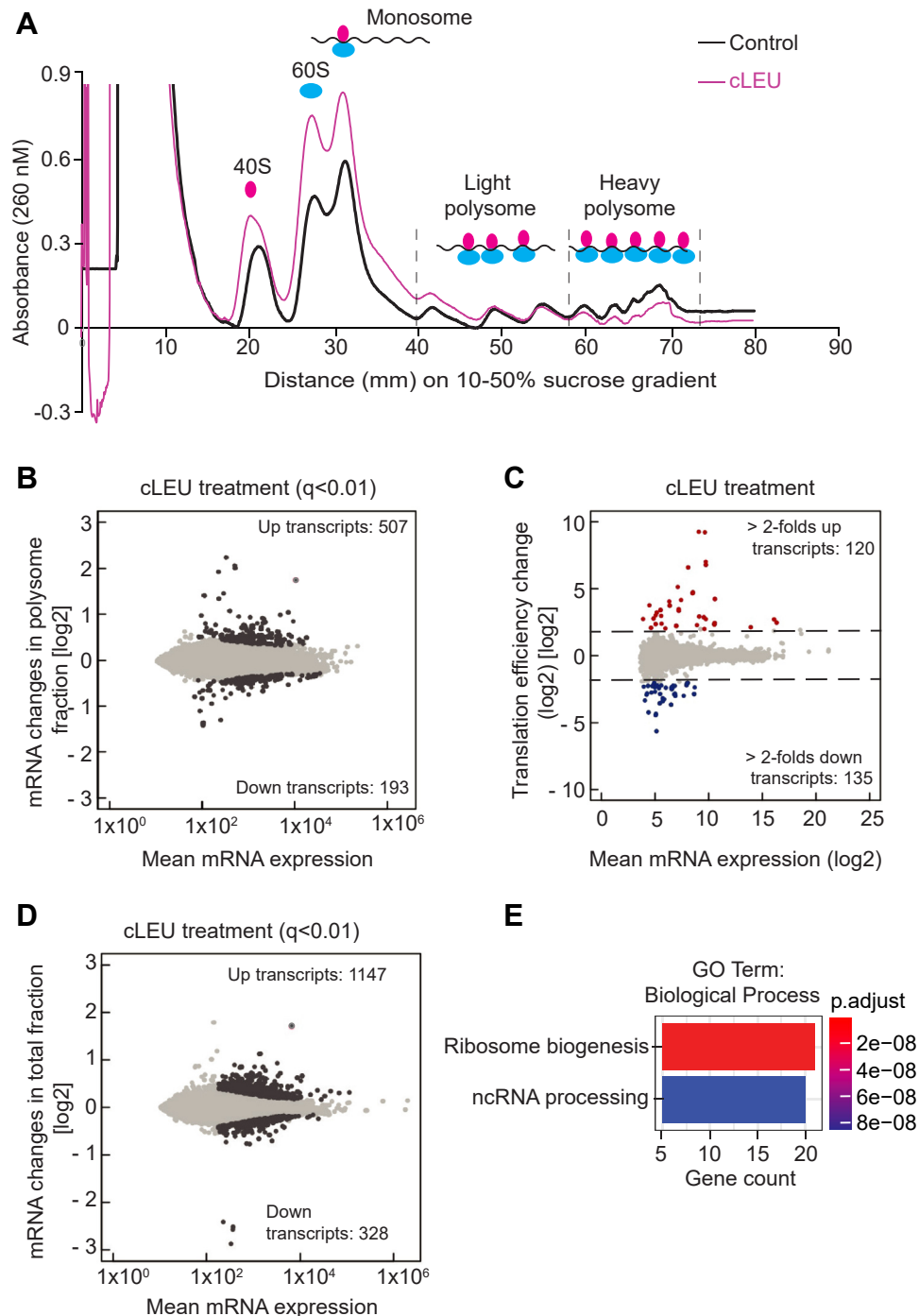


**Figure 3. MAT2A and SAM are essential for maintaining active translation in cells.** *A*, representative merge of polysome curves derived from control (blue) and 6-h cLEU-treated (magenta) cells. The experiment was repeated three times, which resulted in polysome curves with similar morphology. *B*, RNA sequencing was performed using mRNA extracted from the polysome fractions in (*A*). Differential expression analysis was performed for the polysome-bound transcripts exhibiting ten or more read counts. Differences between the control and treated group were considered significant when  $q$  value was smaller than 0.01. *C*, translation efficiency (TE) of each transcript was calculated by a ratio of reads number between the polysome fraction in (*B*) and total RNA. Transcripts exhibiting 2-fold (Log2) or more increments are colored red, and those exhibiting 2-fold (Log2) or more decrements are shown in blue. *D*, RNA sequencing was performed using the total cytoplasmic mRNA from the control cells and cells treated with cLEU. Differential expression analysis was performed for the genes exhibiting ten or more read counts. The genes whose expression were significantly altered upon the treatment are indicated in dark gray. Differences between the control and treated group were considered significant when  $q$  value was smaller than 0.01. *E*, Gene ontology analysis of the transcriptionally downregulated genes shown in (*D*). Two significantly enriched terms ( $p.adjust. < 0.01$ ) are presented in a horizontal bar plot.  $p.adjust.$  adjusted  $p$ -value.  $n = 2$  in all the analyses. cLEU, cycloleucine.

were analyzed by liquid chromatography with tandem mass spectrometry (LC-MS/MS) (Fig. 4A). Coomassie Brilliant Blue (CBB) staining (Fig. 4B) and Western blotting (Fig. 4C) of the

purified protein showed that the purification successfully enriched proteins interacting with FB-MAT2A. We found that 81 proteins were specifically copurified with FB-MAT2A

## mTORC1-independent translation control by MAT2A and SAM

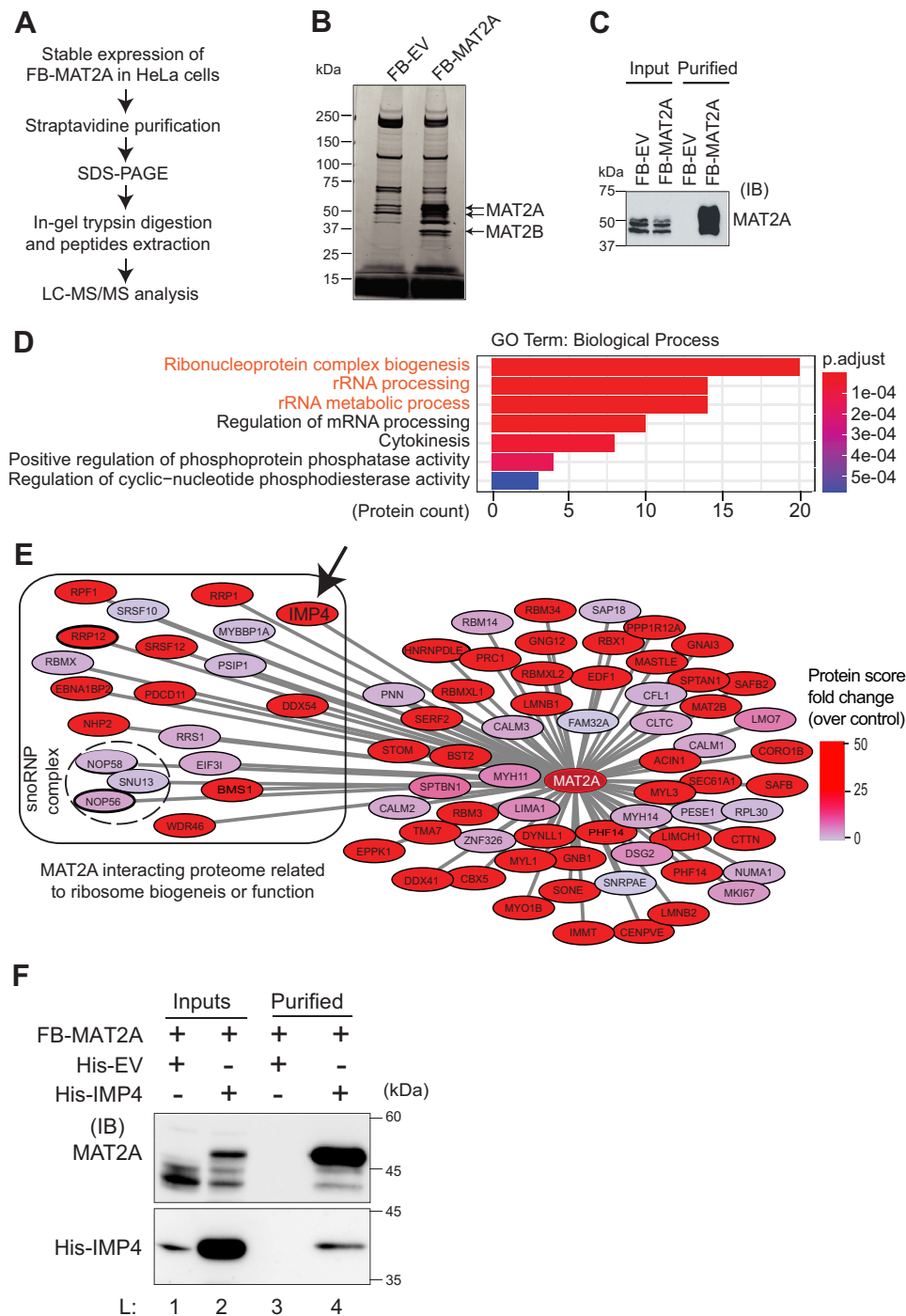


**Figure 4. MAT2A interacts with proteins involved in ribosome biogenesis and translation.** *A*, schematic representation of the workflow for ectopic expression and purification of FB-MAT2A for LC-MS/MS analysis. *B*, FB-MAT2A and its interacting proteins were visualized by Coomassie Brilliant Blue (CBB) staining following SDS-PAGE. *C*, confirmation of purification of FB-MAT2A by Western blot using a monoclonal MAT2A antibody. *D*, Gene ontology (GO) analysis for the FB-MAT2A interacting proteins. Top seven enriched terms are presented in a horizontal bar blot for GO-term Biological Process. The color grades indicate the adjusted *p*-value for each enriched term. *E*, FB-MAT2A interacting proteins are presented as a network. The color grade indicates the fold change of protein score over control purification. The proteins in the left rectangular area are related to ribosome biogenesis or function. Proteins inside the dashed black circle are the components of the snoRNP complex. The IMP4 protein is indicated by a black arrow. *F*, copurification of His-IMP4 with FB-MAT2A by streptavidin affinity purification. The Western blotting was done using monoclonal mouse anti-MAT2A and polyclonal rabbit anti-His tag antibodies.

(Table S2). In the result of GO analysis, the top enriched terms were related to ribosome biogenesis and/or functions such as ribonucleoprotein complex biogenesis, rRNA processing, rRNA metabolic process, preribosome, small nucleolar ribonucleoprotein complex, and snoRNA binding (Figs. 4D and S3,

A and B), suggesting an involvement of MAT2A in ribosome biogenesis and/or ribosome function. Notably, the core protein components of the snoRNP complex (NOP56, NOP58 and SNU13), except for FBL (Fibrillarlin), were found in the purified proteins (Fig. 4E). The snoRNP complex plays an

important role in ribosome biogenesis by 2'-O-methylation of rRNA, and this methylation also enhances the translation capability of ribosome (56). These results strongly support the imperativeness of MAT2A in the ribosome function.

### **MAT2A is required for rRNA processing**

Mammalian ribosomal RNA is transcribed as a single large transcript called the 47S pre-rRNA. This pre-rRNA bears external and internal transcribed spacers (ITSs), which must be removed by the complex process of endonucleolytic and exonucleolytic cleavages at specific sites to produce the mature 18S, 5.8S, and 28S rRNAs (57) (Fig. S4A). Among the MAT2A-interacting ribosome biogenesis factors, we further confirmed the interaction of IMP4 with MAT2A by copurification of poly-histidine-tagged IMP4 (His-IMP4) with FB-MAT2A (Fig. 4F). IMP4 is a component of the small subunit processome. The small subunit processome mediates 18S rRNA maturation by cleavage at A0, A1, and A2 sites (58). To elucidate whether MAT2A is required for the pre-rRNA transcription, we quantified the pre-rRNA content in *Mat2a*-knocked-down Hepa1 cells by qPCR using a primer pair targeting the 5' external transcribed spacer sequence (59). We observed that *Mat2a* knockdown did not alter the rRNA transcription in Hepa1 cells (Fig. S4B), suggesting that MAT2A is dispensable for rRNA transcription. MAT2A interacted with the snoRNP complex which plays a critical role in rRNA methylation and maturation (60–62) (Fig. 4E). We also observed the interaction of MAT2A with IMP4, one of the 18S rRNA cleavage factors. These observations led to a hypothesis that MAT2A might be involved in rRNA maturation. Indeed, *Mat2a* knockdown decreased the 18S/28S rRNA ratio with reduced production of the 18S rRNA (Fig. 5, A and B). Chemical inhibition of MAT2A by cLEU also reduced the 18S/28S ratio in a concentration-dependent manner (Figs. 5C and S4C). Alterations in rRNA processing were further investigated by measuring the major pre-rRNA stages by Northern blot using ITS1 and ITS2. The reduced production 18S rRNA upon the cLEU treatment was supported by the result that a weakened signal of 18S-E, the immediate precursor of the mature 18S rRNA, was detected using the ITS1 probe (Fig. 5D, Panel 1). Interestingly, we observed a prominent accumulation of 30S and 32S pre-rRNAs, the precursors of the mature 18S rRNA (Fig. 5D, Panels 1 and 2). The decreased 18S rRNA was also observed (Fig. 5D, Panel 3). Considering that rRNA transcription was not affected by MAT2A knockdown, the reduced production of the 18S rRNA could be a result of disturbed 18S rRNA processing. These observations suggest that MAT2A is involved in 18S rRNA cleavage and processing. Insufficient 18S rRNA maturation may have partially contributed to the reduction of protein synthesis upon MAT2A depletion or inhibition.

### **MAT2A contributes to dynamic methylation of proteins involved in translation**

Many proteins involved in translation are methylated in *E. coli*, yeast, and mammals (49, 51, 63–66). Although some of

these methylations appeared important for translation (50, 51, 67), the biological significance of the majority is unclear. Therefore, we hypothesized that a reduction of methylation of proteins involved in translation might cause the protein synthesis reduction upon MAT2A inhibition. To compare methylation of proteins upon MAT2A inhibition, we employed a variant approach of stable isotope labeling by amino acid in cell culture (SILAC) named heavy methyl SILAC (68) followed by identification and quantification of methylated peptides using LC-MS/MS. HeLa cells were labeled with either light or heavy methionine for six generations. The heavy-labeled cells were treated with 30 mM cLEU for 6 h and the light and heavy-labeled cells were then mixed at a ratio of 1:1. Then, ribosomes were purified by two methods for the maximum coverage (Fig. 6A): by immunoprecipitation (IP) (method 1) or ultracentrifugation in sucrose cushion (method 2). In method 1, cells were transfected with the 3× FLAG-tagged RPL23A protein (FL-RPL23A) expression vector and then ribosome containing the FL-RPL23A protein was purified by anti-FLAG IP. For comparison, a mock purification was also performed in parallel using cells transfected with the empty vector (Fig. S5, A and B). In method 2, ribosome was pelleted by passing the cleared lysate through 1 M sucrose cushion in ultracentrifugation (Fig. S5, C and D). We noticed that many ribosomal proteins were purified in both methods (Table S3). By combining the data obtained from the two methods, we identified 28 methylated peptides (Table S3; Sheet 3). After calculating the heavy/light ratio from the relative abundance of methylated peptides, the values were normalized to those of unmethylated methionine-containing peptides derived from the same protein to exclude the possible variability due to the difference in cell number or protein amount between light-labeled and heavy-labeled cells. When no unmethylated methionine-containing peptide was identified in the same protein, the normalization was done using RPL23A (method 1) or PABPC1 (method 2) as the standards (see Supplementary Method for details) (Table S3). By taking average abundance values of peptides purified twice, we finally identified 16 unique peptides (Table S3; Sheet 5). Among the unique peptides, 12 peptides were derived from proteins involved in translation, and five of them showed a reduction by 60% or more in methylation upon MAT2A inhibition by the cLEU treatment for 6 h (Fig. 6B and Table S3). The relative abundance of methionine-containing peptides used for normalization showed a linear correlation in both methods (Fig. 6, C and D), indicating that the same amount of proteins were purified from the control and treatment samples. These results suggest that MAT2A contribute to dynamic methylation of a specific set of proteins for translation.

The highest methylation reduction was observed in K55me2 of eEF1A1 and/or eEF1A2. The chromatogram and mass spectrum of eEF1A1/2K55me2 light and heavy peptides are presented in Figure 7A. We further validated the effect of MAT2A on eEF1A1/2K55me2 by Western blot using a specific antibody for this methylation. For convenience of transfection, we selected HEK293T cells for this experiment.

## mTORC1-independent translation control by MAT2A and SAM

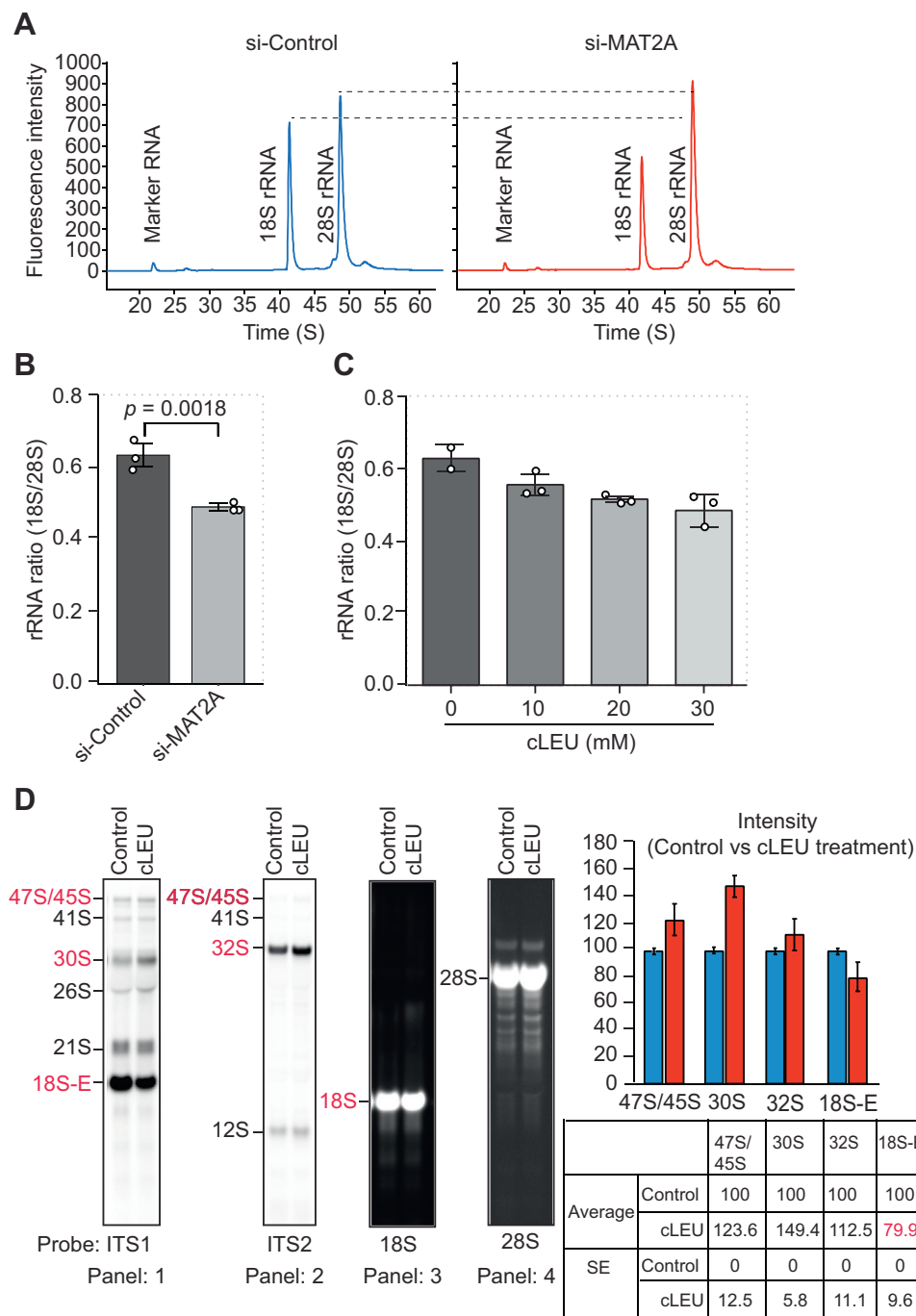


**Figure 5. MAT2A is required for rRNA processing.** A and B, the mature 18S and 28S rRNA were quantified after knockdown of MAT2A in Hepa1 cells. The representative electropherograms from triplicated samples are presented in (A). A bar plot showing a significant reduction of the 18S/28S rRNA ratio is presented in (B). Mean  $\pm$  SD are shown ( $n = 3$  replicates of samples). C, the decreased 18S/28S rRNA ratio was also observed in HeLa cells after chemical inhibition of MAT2A by cLEU. D, panel 1 and 2: Northern blotting showing different pre-rRNA detected by the ITS1 and ITS2 probes. Panel 3 and 4: The mature 18S and 28S rRNAs are detected by specific probes. The bar plot on the right side and the table below indicate the relative quantity of each pre-rRNA that was changed upon cLEU treatment. cLEU, cycloleucine; IP, immunoprecipitation; ITS, internal transcribed spacers.

Because of its ubiquitous expression (69), the principal form of eEF1A in HEK293T cells is eEF1A1. Therefore, we examined the methylation status of eEF1A1K55me2 in HEK293T cells upon MAT2A transient overexpression. First, we validated the specific reactivity of commercially available DiMethyl-eEF1A-K55 antibody (anti-eEF1AK55me2) by overexpressing either wildtype FB-eEF1A1 or mutant FB-eEF1A1K55R (lysine was replaced by arginine) in HEK293T

cells followed by IP with the FLAG antibody and immunoblotting with the anti-eEF1AK55me2 antibody. We observed that the anti-eEF1AK55me2 antibody detected wildtype FB-eEF1A1 both in the input (Fig. 7B, lane 2) and IP (Fig. 7B, lane 5) samples but failed to detect the corresponding signal of FB-eEF1A1K55R (Fig. 7B, Lanes 3 and 6, respectively), corroborating that this antibody specifically detects eEF1A1K55me2. Next, we co-expressed either wildtype FB-

## mTORC1-independent translation control by MAT2A and SAM

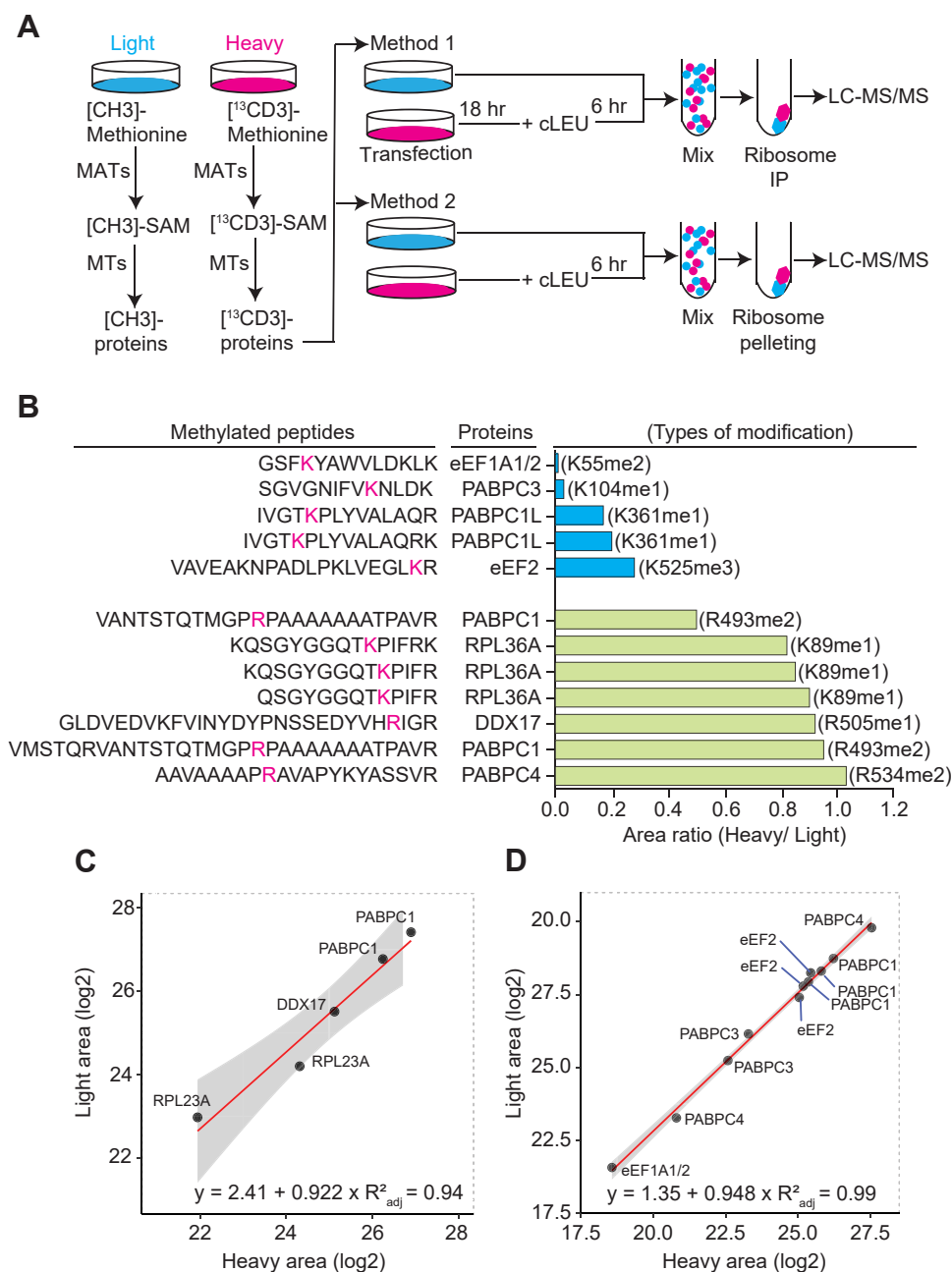


**Figure 6. MAT2A contributes to dynamic methylation of proteins involved in translation.** *A*, schematic diagram of heavy methyl-SILAC and purification of ribosomes by IP (method 1) or by pelleting in ultracentrifugation (method 2). *B*, the identified methylated peptides derived from proteins involved in translation are shown. The methylated residues are shown in *magenta*. The *horizontal bar plot* indicates the heavy/light ratio of each peptide. A ratio smaller than 1 indicates reduced methylation in the peptide by cLEU treatment. The bars of peptides whose methylation was reduced by more than 60% (ratio < 0.6) are presented in *blue*. The type of modification is labeled at the tip of each bar. Kme1, monomethylated lysine; Kme2, dimethylated lysine; Kme3, trimethylated lysine; Rme1, monomethylated arginine; Rme2, dimethylated arginine. *C* and *D*, correlation analysis between the relative abundance of light and heavy unmethylated methionine-containing peptides used for normalization in methods 1 and 2 are shown in *C* and *D*, respectively (two peptides from PABPC1, two from RPL23A, and one from DDX17 in *C* and one peptide from eEF1A1/2, three from eEF2, three from PABPC1, two from PABPC3, and one from PABPC4 in *D*). The *gray zone* indicates the 95% confidence level interval predicted from a linear model ("lm") in R. cLEU, cycloleucine; IP, immunoprecipitation; MAT, methionine adenosyltransferase; SILAC, stable isotope labeling by amino acid in cell culture.

eEF1A1 or mutant FB-eEF1A1K55R with MAT2A in HEK293T cells. As expected, we observed that the expression of MAT2A increased eEF1A1K55me2 (Fig. 7C, lane 5). This observation was consistent with the reduction in eEF1AK55me2 upon MAT2 inhibition observed in the heavy methyl-SILAC experiments.

### Discussion

In this study, we examined the role of MAT2A in protein synthesis in mammalian cells. We revealed that MAT2A and SAM are essential to maintain global protein synthesis independently of the mTORC1 signaling. In the polysome profiling experiment, we observed that inhibition of the MAT2A activity

## mTORC1-independent translation control by MAT2A and SAM

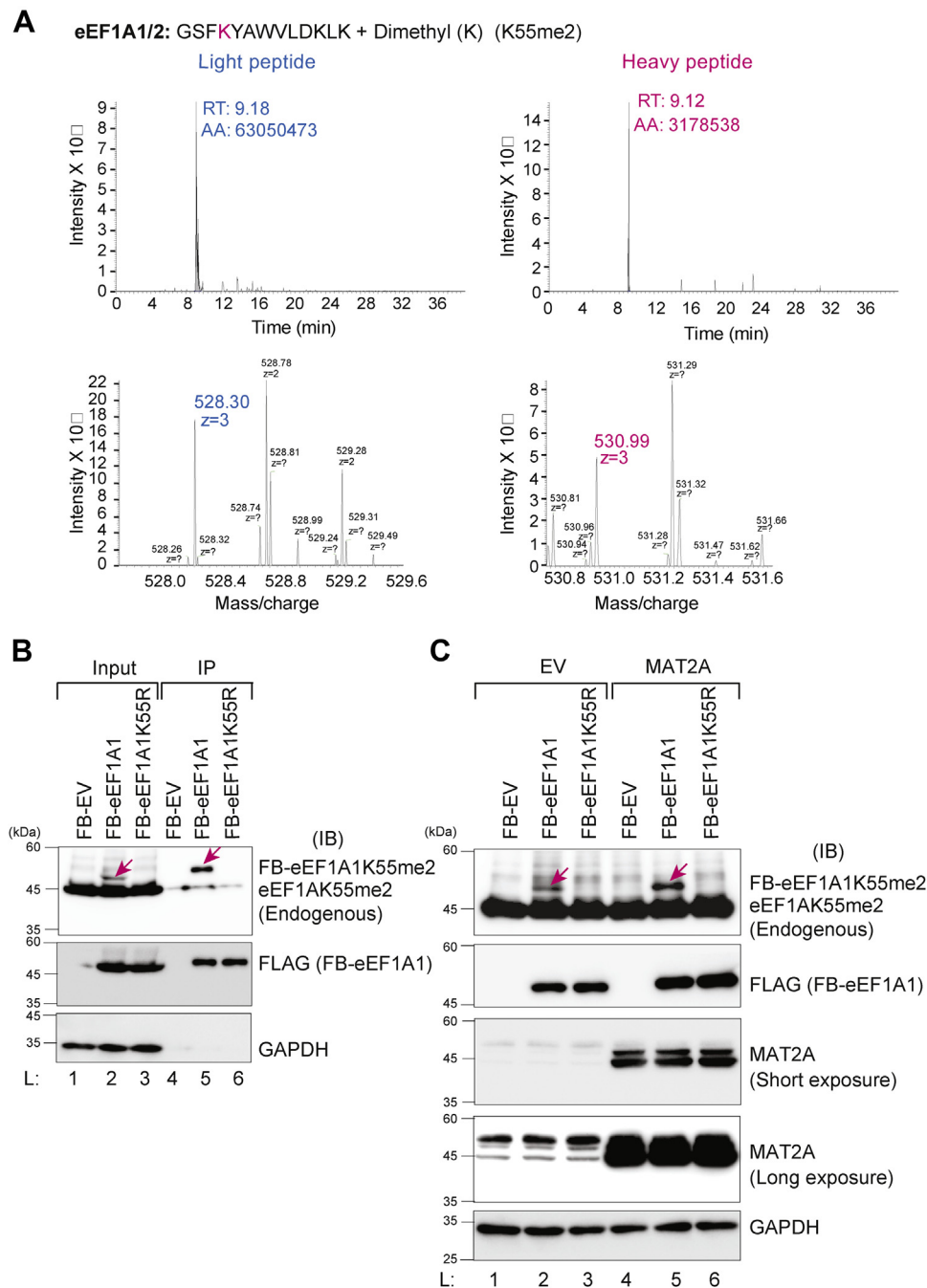


**Figure 7. MAT2A induces methylation of eEF1A1 at lysine 55.** *A*, the chromatogram (*upper panels*) and mass spectrum (*lower panels*) of light and heavy eEF1A1/2K55me2 peptides are presented. The retention time (RT), area (AA), and *m/z* of this peptide are presented in *blue* (light peptide) and *magenta* (heavy peptide). *B*, the specific reactivity of the anti-eEF1AK55me2 antibody was determined. The eEF1A1 WT and the methylation-mutant protein were transiently expressed for 24 h in HEK293T cells, and IP and immunoblotting were done using the indicated antibodies. The *magenta arrows* indicate ectopic FB-eEF1A1. *C*, the eEF1A1 WT and methylation-mutant proteins were co-expressed with MAT2A in HEK293T cells for 24 h, and immunoblotting with the indicated antibodies was done. The *magenta arrows* indicate ectopic FB-eEF1A1. This experiment was repeated two times, which resulted in the same observation.

impaired the formation of active polysome and altered TE of a subset of mRNA. To understand the mechanistic aspects, we studied the MAT2A interactomes by mass spectrometry. We observed that MAT2A interacts with many rRNA processing and ribosome biogenesis factors. We revealed that the 18S rRNA maturation was severely affected by MAT2A depletion and inhibition. By quantitative mass spectrometry, we showed a drastic reduction of methylation of translation factors including

eEF1A1 in MAT2A-inhibited cells. To sum up, MAT2A and SAM promote translation in mammalian cells by (i) facilitating rRNA processing, (ii) promoting active polysome formation, and (iii) regulating methylation of translation factors (Fig. 8). Importantly, the effect of MAT2A and SAM on translation is independent of the mTORC1 signaling.

We observed a reduction in protein synthesis not only upon MAT2A depletion but also by chemical inhibition of MAT2A

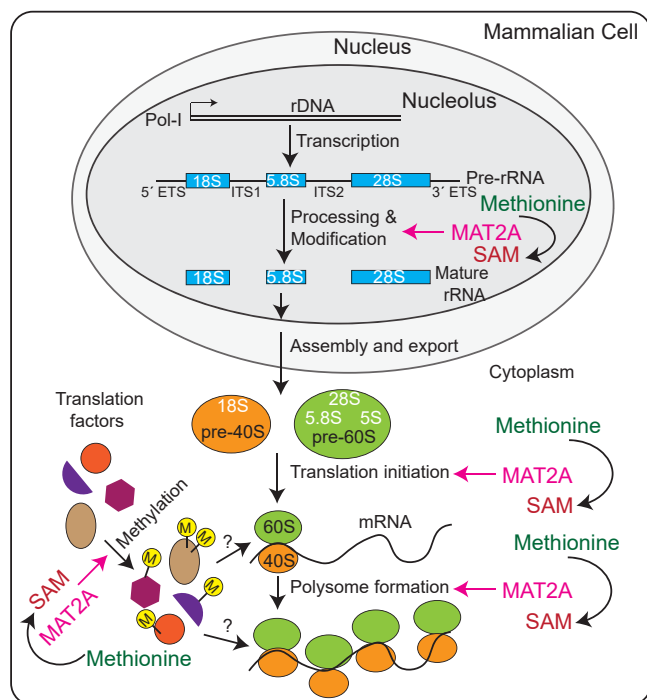


**Figure 8. MAT2A contributes to translation by multipronged mechanisms: promotion of rRNA processing in the nucleolus, promotion of translation initiation and active polysome formation in the cytoplasm, and dynamic methylation of some translation factors.** ITS, internal transcribed spacers; SAM, S-adenosylmethionine.

activity, indicating that MAT2A relies on SAM for promoting protein synthesis. It has been reported that SAM and its precursor methionine are necessary for proliferation of cancer cells (70–72) and stem cells (73–75). Moreover, SAM scarcity in cancer leads to cell cycle arrest in G1 and G2 phases where cells synthesize proteins, lipids, and other biomolecules (76, 77). In addition, cell proliferation requires the synthesis of a copious amount of protein. Therefore, our data suggest that MAT2A and SAM contribute to cell proliferation by maintaining protein synthesis. On the other hand, several studies have depicted that an excess of exogenous SAM supplementation can be toxic and suppresses proliferation of cell lines from various cancers including uterine cervix (78), colon (79), colorectal (80), and breast (81) by arresting cell cycle in S phase (80, 82). Therefore, an optimum amount of SAM is necessary for protein synthesis and cell cycle progression.

In this study, we found that MAT2A regulates translation independently of the mTORC1 activity. Contrary to our findings, a previous study showed that the activity of mTORC1 is highly dependent on cellular SAM concentration. It was reported that when SAM becomes low in HEK293T cells, SAMTOR inhibits the mTORC1 activity by forming a stable dimer with GATOR1. Under a sufficient SAM condition, SAM binds to SAMTOR to disrupt the SAMTOR-GATOR1 complex, thereby activating mTORC1 and translation (33). While our findings are contradictory to this report, the difference may be caused by the SAM depletion techniques employed. They carried out methionine restriction for 2 h in their experiment. The activation of mTORC1 requires its localization on the lysosomal surface, where the activator RHEB

resides, and the localization is stimulated by an amino acid signaling (28, 83). Therefore, the observation by Gu *et al.* might be confounded by a compromised amino acid signaling rather than solely depending on SAM concentration. Further studies are required to clarify these possibilities. It should be noted that serum stimulation increased MAT2A protein (Fig. 1C). This observation may suggest that mTOR induces the expression of MAT2A.

Paradoxically to the drastic protein synthesis reduction, TE of only a small number of transcripts was decreased in MAT2A-inhibited cells. This observation can be explained by the fact that MAT2A is important for global translation rather than that of specific mRNA. Therefore, a small reduction of TE, which was not considered for calculation in Figure 3C, for many genes combinedly might lead to the huge protein synthesis reduction.

The MAT2A-interacting proteins included many rRNA and ribosome biogenesis factors, particularly the components of the snoRNP complex, which mediates rRNA methylation (Fig. 4E). We confirmed the interaction of MAT2A with IMP4. In addition, the 18S rRNA processing was reduced upon MAT2A depletion (Fig. 5, A and B) or inhibition (Fig. 5, C and D), whereas rRNA transcription was not affected (Fig. S4B). The necessity of methylation for rRNA biogenesis (61, 84–86) suggests that the 18S rRNA defects observed upon MAT2A depletion or inhibition are explained by impaired methylation. The interaction of MAT2A with the snoRNP complex may expand the idea of the local SAM synthesis and consumption model of chromatin methylation in which SAM is produced on chromatin for local histone methylation (87, 88). MAT2A may produce SAM for rRNA methylation along with its processing. Further studies including rRNA methylation are necessary to draw an absolute conclusion.

Posttranslational methylation is one of the most common modifications found in a wide range of proteins. Given that translation is one of the critical steps for gene expression control, methylation of ribosomal proteins and translation factors might be crucial for the translational regulation of gene expression. By quantitative mass spectrometry, we revealed that methylation of some translation factors, such as eEF1A1/2K55me2, PABPC3K104me1, PABPC1LK361me1, and eEF2K525me3, were reduced by more than 60% upon MAT2A inhibition (Fig. 6B). We must note that some of these identifications and quantifications may have been disturbed by distinct unmethylated peptides derived from homologous proteins in which amino acid replacements alter the number of the methyl group, such as the replacement of Gly by Ala (see Table S3, sheet 3, column AE). We further validate the effect of MAT2A on eEF1A1K55me2 by using a specific antibody (Fig. 7, B and C); transient overexpression MAT2A induced eEF1A1K55me2. These observations suggest that methylations of these proteins are dynamically altered in response to intracellular SAM concentration.

It has been reported that methylations of some of these proteins are necessary for translation. For example, eEF1AK55me2 is required for protein synthesis and tumorigenesis in lung cancer (51) and cell proliferation in acute

## *mTORC1-independent translation control by MAT2A and SAM*

myeloid leukemia (89). It is also reported that eEF1AK55me2 has a more specific function in enhancing the translation of codons for tryptophan and alanine (90). Therefore, MAT2A may at least partially rely on eEF1AK55me2 to stimulate protein synthesis. eEF2K509me3 (the corresponding residue in human is K525) is essential for maintaining translation frame in yeast (67). Although there is no report of PABPC1L methylation as far as we know, upregulation of PABPC1L is associated with proliferation and migration of prostate and colorectal cancers (91, 92). Therefore, it would be promising to investigate the importance of PABPC1LK361me1 in translation. PABPC3 and PABPC4 are known to be methylated at several lysine and arginine residues (93, 94). However, the biological significance of these methylations is still unknown. Since PABPCs have translation-stimulating capabilities (95–97), the biological significance of their methylations would be promising to be explored in future.

In this study, we focused on methylation of translation-related proteins. tRNA is also highly modified by methylation at different positions, and some of them have already been proven important for various steps of translation (98–100). Therefore, in future, it will be propitious to investigate whether and how MAT2A and SAM contribute to tRNA-modification.

Due to the complex nature of the mTOR signaling, the cancer chemotherapy targeting the mTOR signaling pathways for translation control is often compromised by different mechanisms including mutations of inhibitor binding sites (101, 102), activation of costimulatory molecules (103), induced expression of growth factor receptors (104), and reduced expression of inhibitory molecules (105). Furthermore, the mTOR inhibitors compromise cancer therapy due to their potent immunosuppressive properties (106). Under these circumstances, a therapy targeting MAT2A could be an alternative to suppress the translation for cancer therapy.

### **Experimental procedures**

#### **Cell culture**

Hepa1 and HeLa cells were cultured in Dulbecco's Modified Eagle's Medium (DMEM) containing 4.5 g/l glucose (D5796, DMEM-high glucose, Sigma-Aldrich) supplemented with 10% fetal bovine serum (FBS) (172012, Sigma-Aldrich) and combination of 100 U/ml penicillin and 100 µg/ml streptomycin (15140-122, penicillin-streptomycin, Thermo Fisher Scientific). In polysome analysis, HeLa cells were cultured in DMEM media containing 4.5 g/l glucose (08458-16, Nacalai Tesque) supplemented with 10% FBS (26140079, Thermo Fisher Scientific). HEK293T cells were cultured in DMEM containing 1.0 g/l glucose (D6046, Sigma Aldrich) supplemented with 10% FBS (172012, Sigma Aldrich).

#### **Plasmids**

The pEF1α-FLAG-Biotag empty vector (FB-EV), pEF1α-FLAG-Biotag-MAT2A (FB-MAT2A), and pEF1α-FLAG-Biotag-BirA (FB-BirA) vectors were described in previous studies (87, 107). The pcDNA3.1(+)-RPS2-TEV-3×-FLAG (FL-RPS2)

and pcDNA3.1(+)-RPL23A-TEV-3×-FLAG (FL-RPL23A) vectors were constructed in this study. The human RPS2 (NM\_002952.3) and RPL23A (NM\_000984.5) cDNAs were amplified from HEK293T cells using a forward primer including a BamH1 restriction site and a reverse primer including a TEV protease site followed by the 3× FLAG sequence and an Xho1 restriction site. The amplified cDNAs were then introduced into the pcDNA 3.1 (+) vector at the BamH1 and Xho1 sites. Therefore, the resulting plasmids encode C-terminal 3× FLAG-tagged RPS2 and 3× FLAG-tagged RPL23A. The MSCV-FB-eEF1A1 (FB-eEF1A1) and MSCV-FB-eEF1A1K55R mutant (FB-eEF1A1K55R) plasmids were constructed in this study. Human eEF1A1 cDNA (NM\_001402.5) was PCR-amplified using cDNA from the ASPC1 cell line and was inserted into the MSCV vector using its BamH1 restriction site. The MSCV-FB-eEF1A1K55R mutant vector was then constructed by introducing the point mutation to the MSCV-FB-eEF1A1 plasmid. To construct the pcDNA-IMP4-His (His-IMP4) plasmid, human IMP4 cDNA was PCR-amplified from the human brain cDNA library (Human Brain, Hypothalamus Marathon-Ready cDNA, No. 639329, Takara Bio). The amplified cDNA was then inserted into the HindIII and SacII sites of the pcDNA 3.1/myc-His B vector (V800-20; ThermoFisher Scientific).

#### **Western blot analysis**

Western blot analysis was performed as described in previous studies with modifications (78, 87). Briefly, cells were lysed by 1× SDS sample buffer (62.5 mM Tris-HCl pH 6.8, 1% SDS, 10% glycerol, 1% 2-mercaptoethanol and 0.02% bromophenol blue) containing protease inhibitors (0469315900, cOmplete Mini EDTA-free Protease Inhibitor Cocktail Tablets, Roche) or by radioimmunoprecipitation assay buffer (50 mM Tris-HCl pH 7.4, 150 mM NaCl, 1 mM EDTA, 1% NP-40, 0.5% Na-deoxycholate, 0.1% SDS and cOmplete protease inhibitors). For detection of phosphorylated proteins, the cell lysis buffer additionally contained a phosphatase inhibitor (04906837001, PhosSTOP, Roche). Protein amount was quantified by either a protein assay kit (22660, Pierce 660 nm protein assay reagent, Thermo Fisher Scientific) or SDS-PAGE followed by CBB (50% methanol, 10% acetic acid and 0.1% R-250 or G-250) staining and quantification of stain density with an ImageJ software (version 1.53i). The extracted protein was denatured by heating at 95 °C for 5 min in the presence of the SDS-PAGE sample buffer. The protein was separated by SDS-PAGE in an 11% polyacrylamide gel (15% for SUnSET and ribosomal proteins). The separated proteins were then transferred to 0.45-µm PVDF membrane (IPVH00010, Immobilon-P Transfer Membrane, Merck Millipore). After transfer, the PVDF membranes were blocked in 3 to 5% skim milk in TBS-T (50 mM Tris-HCl pH 7.5, 150 mM NaCl and 0.05% Tween 20) before incubation with antibodies. When phosphorylated proteins were examined, antibody reactions were done in TBS-T containing 3% BSA. The imaging was done by a ChemiDoc MP imaging system (Bio-Rad Laboratories) using Clarity Western ECL Substrate (1705060, Bio-Rad

Laboratories). The information on antibodies is provided in the “[Supplementary Method](#)” section.

### **Translation assay**

The translation rate was examined by SUnSET (52). Cells were grown to 70 to 80% confluency and pulse-labeled with 20 mg/ml puromycin (P8833, Puromycin dihydrochloride, Sigma-Aldrich) for 30 min at 37 °C in a cell culture incubator. In serum stimulation, cells were grown in serum-free DMEM containing 4.5 g/l glucose (D5796, Sigma-Aldrich) for a period of 24 h. Then, cells were returned into DMEM supplemented with 10% FBS for 1 h or 3 h before pulse labeling with puromycin. Cells were lysed in radioimmunoprecipitation assay buffer supplemented with the protease inhibitors. Around 1 to 1.5 µg of total clarified lysate protein was loaded in a lane for SDS-PAGE and subsequent Western blotting detection was done by using an antipuromycin antibody.

### **Polysome analysis**

Approximately  $5 \times 10^6$  cells were seeded in 25 ml of media in 15-cm cell culture dishes and were grown for 18 h. The cells in the treatment group were then treated with 30 mM cLEU (A48105-10G, Sigma-Aldrich) for 6 h, and the cells were harvested 24 h after the seeding. The polysome was stabilized by treating with 100 µg/ml CHX (06741-04, Nacalai Tesque) for 10 min. The harvested cells were lysed in 550 µl of hypotonic lysis buffer (10 mM Hepes-KOH pH 7.9, 1.5 mM MgCl<sub>2</sub>, 10 mM KCl, 0.5 mM DTT, 1% Triton X-100, 100 µg/ml CHX, 40 U/ml RNasin, and cOmplete protease inhibitor). The lysate was cleared by centrifugation at 15,000g for 10 min. A total of 500 µl of lysate containing around 150 µg of total RNA was layered on 10 to 50% sucrose gradient in polysome buffer (20 mM Hepes-KOH pH 7.6, 5 mM MgCl<sub>2</sub>, 100 mM KCl, 1 mM DTT, and 100 µg/ml CHX) and was centrifuged at 274,000g for 1.5 h at 4 °C (40,000 rpm using an SW41Ti rotor, 331362, Beckman Coulter). A Piston Gradient Fractionator (Biocomb) equipped with a single path UV-1 optical unit (Biomini UV-monitor, ATTO) and a chart recorder (Digital mini recorder, ATTO) was used for sucrose fraction collection and polysome profile generation as previously described (108).

### **RNA sequencing**

The library was prepared using an MGIEasy RNA Directional Library Prep Set (MGI Tech Co, Ltd) following the manufacturer's manual. To examine the prepared library quality, the circularized DNA was prepared using an MGIEasy circularization Kit (MGI Tech Co, Ltd) with the manufacturer's guideline. After making DBA nanoball by a DNBSEQ-G400RS High-throughput Sequencing Kit (MGI Tech Co, Ltd), the sequencing was performed using DNBSEQ-G400. The differential gene expression analysis was performed for transcripts aligned to more than ten reads using estimateSizeFactors function, estimateDispersions function, and nbinomWaldTest function in R package DESeq2.

### **Purification of FB-MAT2A and LC-MS/MS analysis**

Two million stable expression cells were seeded in four 10-cm dishes 24 h before the cell harvest. The harvested cells were lysed in 1 ml of IP buffer (10 mM Tris-HCL pH 7.4, 150 mM NaCl, 1 mM EDTA, 0.3% NP-40, 2 mM DDT, cOmplete protease inhibitor, and PhosSTOP phosphatase inhibitor). The clarified supernatant was used for affinity purification with streptavidin-conjugated magnetic beads (Dynabeads M-280 Streptavidin, Thermo Fisher Scientific) (78, 107). Briefly, the cleared lysate and 20 µl of Dynabeads slurry were incubated with an end-to-end rotation at 4 °C for 2 h. The protein-bound beads were washed, and the proteins were eluted in the presence of biotin at 70 °C for 15 min. The eluted protein was processed for mass spectrometry according to the previously described protocol (109, 110). Briefly, the purified proteins were separated by SDS-PAGE using a 5 to 20% gradient gel (HON-052013; Oriental Instruments Co, Ltd) and were stained with CBB for visualization. Every lane was divided into small gel pieces and the pieces were treated with 30% acetonitrile (ACN) for destaining and then with 50% and 100% ACN for dehydration. The samples were treated with DTT and then with acrylamide for reduction and alkylation of cysteine side chains. The samples were digested with 10 to 30 ng of trypsin (V5280, Trypsin Gold, Promega) in digestion buffer (50 mM ammonium bicarbonate and 10% ACN) overnight at 37 °C. The digested peptides were eluted in a solution containing 75% ACN and 1% formic acid solution. The eluates were then concentrated in SpeedVac and were analyzed in an Orbitrap Fusion mass spectrometer connected with an Easy-nLC 1000 HPLC (Thermo Fisher Scientific). The obtained raw MS/MS data were then converted to mgf files using a Proteome discoverer software (version 1.3.0.339, Thermo Fisher Scientific). The converted files were submitted to the database search for peptide identification using a Mascot search engine (Matrix Science) considering propionamide (Cys) as a fixed modification and acetyl (Protein N-term) and oxidation (Met) as variable modifications. The precursor ion and MS/MS tolerances were set to 5 ppm and 0.5 Da, respectively. A maximum of three miscleavage was allowed without considering nonspecific cleavage. The human proteins in Swissprot (Jan 2018) and a homemade contaminant protein list were searched. The number of proteins included in the searched database were 20,560 in total. The threshold of Mascot expectation value for significant peptide-spectral matches were set to 0.05. The false discovery rates estimated by Mascot decoy search were reported as follows: 162 PSM in decoy database *versus* 6262 in real database (2.63%) for Control IP and 163 *versus* 7169 (2.27%) for FLAG-Bio-MAT2A IP. The result from a single experiment is shown.

### **Quantification of rRNA**

Ribosomal RNA was quantified by a 2100 Bioanalyzer Instrument (Agilent) using an Agilent RNA 6000 Pico kit (5067-1513, Agilent) following the manufacturer's instruction.

## mTORC1-independent translation control by MAT2A and SAM

### Northern blotting

Northern blotting of rRNA precursors was performed according to a previously described protocol (111). Briefly, total RNA was isolated from HeLa cells treated with either cLEU or none by using an RNeasy Plus Mini kit (74134, Qiagen) following the protocol supplied by the manufacturer. Four micrograms of the total RNA were separated by electrophoresis using a 1.2% formaldehyde-agarose denaturing gel in the presence of 1× TT (30 mM Tricine and 30 mM triethanolamine) at 200 V for 120 min. The separated RNA was then transferred to Hybond-N+ membrane (RPN303B, GE Healthcare) by a capillary method in the presence of 20× SSC (3 M NaCl and 300 mM trisodium citrate dihydrate) for 18 h. The RNA was then UV-crosslinked at 120 mJ/cm<sup>2</sup> by using a CL-1000 UV-crosslinker device. The membranes were incubated in the hybridization buffer containing the DIG-labeled hybridization probes at 50 °C for 20 h. The membrane was then washed once in 2× SSC containing 0.1% SDS for 15 min at 50 °C, then twice in 0.1× SSC containing 0.1% SDS for two times at the same temperature, and finally in 1× MA buffer (100 mM maleic acid and 150 mM NaCl, pH 7.0) for 10 min at room temperature. After being blocked by a blocking reagent (11096176001, Roche) for 30 min, the membrane was incubated with anti-digoxigenin-AP, Fab fragments (11093274910, Roche) in the blocking buffer for 1 h. After that, the membrane was washed three times in 1× MA buffer containing 0.3% Tween-20 and then was equilibrated in buffer-A (100 mM Tris-HCl and 100 mM NaCl, pH 9.5). RNA was detected using CDP-star (11759051001, Roche) and a LAS-4000 mini device. The 5' DIG-labeled probes for the detection of the precursor rRNAs are follows:

ITS1: 5'-CCTCGCCCTCCGGGCTCCGGGCTCCGTTAA TGATC-3'

ITS2: 5'-CTGCGAGGGAACCCCGAGCCGCGCA-3'

The mature human 18S and 28S rRNAs were detected by DIG-labeled probes that were synthesized by PCR DIG Probe Synthesis Kit (11636090910, Roche) using the following primers.

18S rRNA: 5'-ATCAAGAACGAAAGTCGGAGGTTTCG-3' and 5'-GTGCAGCCCCGGACATCTAAG-3'.

28S rRNA: 5'-GCCGACTTAGAACTGGTGCGG-3' and 5'-CTCACCGGGTCAGTGAAAAACGA-3'.

### Heavy-methyl SILAC experiment

The heavy methyl-SILAC experiment was conducted based on the principles and procedure described in earlier researches (68, 112, 113). The SILAC labeling media were prepared by reconstituting commercially available DMEM high-glucose media depleted for glutamine, methionine, and cysteine (21013024; DMEM high glucose, no glutamine, no methionine, no cysteine cell culture media, Thermo Fisher scientific). For reconstitution, we added 4 mM glutamine (25030-081, Thermo Fisher scientific), 200 μM cysteine (1001527621, L-cysteine dihydrochloride, Sigma-Aldrich) and either 200 μM normal methionine (1001818815; L-Methionine, Sigma-Aldrich) for the light medium or 200 μM heavy methionine

(CDLM9289025, L-methionine, Methyl-13C 99%, Methyl-D3 98%, Cambridge Isotope Laboratories) for the heavy medium. After reconstitution, we added 10% dialyzed FBS (F0392, Sigma-Aldrich) and a combination of 100 U/ml penicillin and 100 μg/ml streptomycin (15140-122, Penicillin-Streptomycin, Thermo Fisher scientific). HeLa cells were cultured in either light or heavy medium for at least six generations. The heavy-labeled cells were treated with 30 mM cLEU for 6 h before harvest. The ribosome was purified as follows:

#### Method 1 (purification by IP)

Light- and heavy-labeled cells were transfected with 15 μg of either the FL-EV or FL-RPL23A plasmid and were grown for 24 h before harvest. After cell harvest by trypsinization, an equal number of light- and heavy-labeled cells were mixed and were lysed in 700 μl of lysis buffer (10 mM Hepes-KOH pH 7.4, 100 mM NaCl, 10 mM MgCl<sub>2</sub>, 10% glycerol, 2 mM DTT, 1 mM PMSF, 2% NP-40, and cOmplete protease inhibitor). The cleared lysate was then used for ribosome purification by an anti-DDDDK antibody bound to magnetic beads (M185-11R, anti-DDDDK-tag mAb-magnetic beads, MBL) at 4 °C for 2 h. The ribosomes were then heat-eluted and were denatured in the presence of SDS-sample buffer.

#### Method 2 (purification by pelleting on sucrose cushion)

5 × 10<sup>6</sup> of light- and heavy-labeled cells were mixed in 1:1 ratio and were lysed in 350 μl of lysis buffer (20 mM Tris-HCl pH 7.5, 150 mM NaCl, 5 mM MgCl, 1 mM DTT, 1% Triton-X100, cOmplete protease inhibitor, and 100 μg/ml CHX). The lysate was clarified by centrifugation at 2000g for 20 min at 4 °C. The cleared lysate was then layered on 900 μl of 1 M sucrose cushion in a 13 × 56 mm 3.2-ml capacity thick-wall polycarbonate ultracentrifuge tube (362305; Beckman Coulter). The tube was then centrifuged in a TLA-110 fixed angle rotor (366735, Beckman Coulter) at 543,000g (100,000 rpm) for 1 h at 4 °C in an Optima MAX-XP Benchtop Ultracentrifuge (Beckman Coulter). The resulting ribosome pellet was washed with ice-cold PBS, was dissolved in SDS-sample buffer and was denatured at 95 °C for 5 min.

After purification of ribosome by either method, the LC-MS/MS sample preparation and analysis were performed as described in "Purification of FB-MAT2A and LC-MS/MS analysis" except that methylation and demethylation at Lys and Arg and trimethylation at Lys were also included in the variable modifications. The human proteins in Swissprot (Nov 2020) and a homemade contaminant protein list were searched. The number of proteins included in the searched database was 20,692 in total. The threshold of Mascot expectation value for significant peptide-spectral matches was set to 0.05. The false discovery rates estimated by Mascot decoy search were reported as follows: 118 PSM in decoy database *versus* 12,888 in real database (0.92%) for ribosome isolation by ultracentrifugation and 65 *versus* 5025 (1.29%) for FLAG-RPL23a IP. The result from a single experiment is shown. Details in the methylated peptides identification procedure can be found in "Supplementary Method" section.

### Statistical analysis

Welch two-sample *t* test was performed using an R program (Version 4.0.2) for comparison of *Mat2a* mRNA (Fig. S1A) and rRNA ratio (Fig. 5B). The relative intensity values were analyzed by one-way analysis of variance assuming equal variance followed by Tukey's honest significance test for the comparison of multiple means (Fig. 1B). Two sample unpaired *t* test was performed to compare the normalized intensities of puromycin-labeled peptides (Fig. 1C). GO analysis of proteins or genes were performed by using package "Go.db" with "enrichGo" function in R. Pearson correlation analysis was performed to compare the correlation between the abundance of light and heavy unmethylated methionine-containing peptides (Fig. 6, C and D) using package "ggpmic" with "stat(e-q.label)" function in R.

### Data availability

The raw data files of mass spectrometry are available in the MassIVE public database (<https://massive.ucsd.edu/ProteoSAFe/static/massive.jsp>, Dataset ID: MSV000089292 and MSV000089296), and the raw data for mRNA sequencing are available in GEO with ID: GSE201299.

**Supporting information**—This article contains supporting information (59, 87, 88, 114).

**Acknowledgments**—We are thankful to Dr Tadashi Nakagawa, Department of Cell Proliferation, Tohoku University Graduate School of Medicine, for the technical advice on the SUnSET experiment. We are grateful to the members of our laboratory for their useful suggestions and advice. We would like to express our gratitude also to Moeka Seki, Laboratory of Gene Regulation, Tohoku University Graduate School of Pharmaceutical Science for the supply of HeLa cells during the research works. We are also grateful to Dr Kenta Teruya, Associate Professor of the Department of Neurochemistry, Tohoku University Graduate School of Medicine for supplying human cDNA library during gene cloning.

**Author contributions**—M. A., H. S., Y. M., N. C. L., T. S., N. S., R. N., S. H., L. L., M. K. K., and Y. K. investigation; M. A. writing-original draft; H. S., K. I., and T. I. supervision; H. S., K. I., and T. I. writing-review and editing; N. C. L., M. M., T. I., and K. I. formal analysis; Y. I. and T. S. resources.

**Funding and additional information**—This study has been supported by Grants-in-Aid for Scientific Research from the Japan Society for the Promotion of Science (22H00443, 20KK0176 and 18H04021 to K. I., 18H03977 to T. I., 20K07321 to H. S., and 19K07680 and 16K07108 to M. M.), Research Grant in the Natural Sciences from the Mitsubishi Foundation (to K. I.), AMED under Grant Number JP19gm1110010 (T. I.) and Platform Project for Supporting Drug Discovery and Life Science Research (Basis for Supporting Innovative Drug Discovery and Life Science Research [BINDS]) from AMED under Grant Numbers JP21am0101078 and JP22ama121008 (to Y. K.).

**Conflict of interest**—The authors declare that they have no conflicts of interest with the contents of this article.

**Abbreviations**—The abbreviations used are: 4E-BP, 4E binding protein; ACN, acetonitrile; CBB, Coomassie Brilliant Blue; CHX, cycloheximide; cLEU, cycloleucine; DMEM, Dulbecco's Modified Eagle's Medium; eIF4A, eukaryotic initiation factor 4A; eIF4B, eukaryotic initiation factor 4B; FB-MAT2A, FLAG-Bio-tagged MAT2A; FBS, fetal bovine serum; IP, immunoprecipitation; ITSs, internal transcribed spacers; MAT, methionine adenosyltransferase; mTORC1, mechanistic target of rapamycin complex 1; S6K, S6 kinase; SAM, S-adenosylmethionine; SILAC, stable isotope labeling by amino acid in cell culture; TE, translation efficiency.

### References

- Buttgereit, F., and Brand, M. D. (1995) A hierarchy of ATP-consuming processes in mammalian cells. *Biochem. J.* **312**, 163–167
- Rolfe, D. F., and Brown, G. C. (1997) Cellular energy utilization and molecular origin of standard metabolic rate in mammals. *Physiol. Rev.* **77**, 731–758
- Verduyn, C., Stouthamer, A. H., Scheffers, W. A., and van Dijken, J. P. (1991) A theoretical evaluation of growth yields of yeasts. *Antonie Van Leeuwenhoek* **59**, 49–63
- Topisirovic, I., and Sonenberg, N. (2011) mRNA translation and energy metabolism in cancer: the role of the MAPK and mTORC1 pathways. *Cold Spring Harb. Symp. Quant. Biol.* **76**, 355–367
- Boroughs, L. K., and DeBerardinis, R. J. (2015) Metabolic pathways promoting cancer cell survival and growth. *Nat. Cell Biol.* **17**, 351–359
- Vander Heiden, M. G., Cantley, L. C., and Thompson, C. B. (2009) Understanding the Warburg effect: the metabolic requirements of cell proliferation. *Science* **324**, 1029–1033
- Ma, X. M., and Blenis, J. (2009) Molecular mechanisms of mTOR-mediated translational control. *Nat. Rev. Mol. Cell Biol.* **10**, 307–318
- Roux, P. P., and Topisirovic, I. (2018) Signaling pathways involved in the regulation of mRNA translation. *Mol. Cell Biol.* **38**, e00070-18
- Sonenberg, N., and Hinnebusch, A. G. (2009) Regulation of translation initiation in eukaryotes: mechanisms and biological targets. *Cell* **136**, 731–745
- Jefferies, H. B., Reinhard, C., Kozma, S. C., and Thomas, G. (1994) Rapamycin selectively represses translation of the "polypyrimidine tract" mRNA family. *Proc. Natl. Acad. Sci. U. S. A.* **91**, 4441–4445
- Dorrello, N. V., Peschiaroli, A., Guardavaccaro, D., Colburn, N. H., Sherman, N. E., and Pagano, M. (2006) S6K1- and betaTRCP-mediated degradation of PDCD4 promotes protein translation and cell growth. *Science* **314**, 467–471
- Faller, W. J., Jackson, T. J., Knight, J. R. P., Ridgway, R. A., Jamieson, T., Karim, S. A., et al. (2015) mTORC1-mediated translational elongation limits intestinal tumour initiation and growth. *Nature* **517**, 497–500
- Proud, C. G. (2019) Phosphorylation and signal transduction pathways in translational control. *Cold Spring Harb. Perspect. Biol.* **11**, a033050
- Raught, B., Peiretti, F., Gingras, A.-C., Livingstone, M., Shahbazian, D., Mayeur, G. L., et al. (2004) Phosphorylation of eucaryotic translation initiation factor 4B Ser422 is modulated by S6 kinases. *EMBO J.* **23**, 1761–1769
- Bhat, M., Robichaud, N., Hulea, L., Sonenberg, N., Pelletier, J., and Topisirovic, I. (2015) Targeting the translation machinery in cancer. *Nat. Rev. Drug Discov.* **14**, 261–278
- de la Parra, C., Walters, B. A., Geter, P., and Schneider, R. J. (2018) Translation initiation factors and their relevance in cancer. *Curr. Opin. Genet. Dev.* **48**, 82–88
- Truitt, M. L., and Ruggero, D. (2016) New frontiers in translational control of the cancer genome. *Nat. Rev. Cancer* **16**, 288–304
- Robichaud, N., del Rincon, S. V., Huor, B., Alain, T., Petruccioli, L. A., Hearnden, J., et al. (2015) Phosphorylation of eIF4E promotes EMT and metastasis via translational control of SNAIL and MMP-3. *Oncogene* **34**, 2032–2042
- Ruggero, D. (2013) Translational control in cancer etiology. *Cold Spring Harb. Perspect. Biol.* **5**, a012336

## mTORC1-independent translation control by MAT2A and SAM

20. Silvera, D., Formenti, S. C., and Schneider, R. J. (2010) Translational control in cancer. *Nat. Rev. Cancer* **10**, 254–266
21. Martineau, Y., Azar, R., Müller, D., Lasfargues, C., El Khawand, S., Anesia, R., et al. (2014) Pancreatic tumours escape from translational control through 4E-BP1 loss. *Oncogene* **33**, 1367–1374
22. Zhang, L., Pan, X., and Hershey, J. W. B. (2007) Individual over-expression of five subunits of human translation initiation factor eIF3 promotes malignant transformation of immortal fibroblast cells. *J. Biol. Chem.* **282**, 5790–5800
23. Tian, T., Li, X., and Zhang, J. (2019) mTOR signaling in cancer and mTOR inhibitors in solid tumor targeting therapy. *Int. J. Mol. Sci.* **20**, 755
24. Xie, J., Wang, X., and Proud, C. G. (2016) mTOR inhibitors in cancer therapy. *F1000Res.* **5**, F1000 Faculty Rev-2078
25. Zou, Z., Tao, T., Li, H., and Zhu, X. (2020) mTOR signaling pathway and mTOR inhibitors in cancer: progress and challenges. *Cell Biosci.* **10**, 31
26. Hua, H., Kong, Q., Zhang, H., Wang, J., Luo, T., and Jiang, Y. (2019) Targeting mTOR for cancer therapy. *J. Hematol. Oncol.* **12**, 71
27. Bozulic, L., and Hemmings, B. A. (2009) PIKKing on PKB: regulation of PKB activity by phosphorylation. *Curr. Opin. Cell Biol.* **21**, 256–261
28. Kim, E., Goraksha-Hicks, P., Li, L., Neufeld, T. P., and Guan, K.-L. (2008) Regulation of TORC1 by Rag GTPases in nutrient response. *Nat. Cell Biol.* **10**, 935–945
29. Park, E., Park, J., Han, S.-W., Im, S.-A., Kim, T.-Y., Oh, D.-Y., et al. (2011) NVP-BKM120, a novel PI3K inhibitor, shows synergism with a STAT3 inhibitor in human gastric cancer cells harboring KRAS mutations. *Int. J. Oncol.* **40**, 1259–1266
30. Rastogi, R., Jiang, Z., Ahmad, N., Rosati, R., Liu, Y., Beuret, L., et al. (2013) Rapamycin induces mitogen-activated protein (MAP) kinase phosphatase-1 (MKP-1) expression through activation of protein kinase B and mitogen-activated protein kinase pathways. *J. Biol. Chem.* **288**, 33966–33977
31. Wang, X., Hawk, N., Yue, P., Kauh, J., Ramalingam, S. S., Fu, H., et al. (2008) Overcoming mTOR inhibition-induced paradoxical activation of survival signaling pathways enhances mTOR inhibitors' anticancer efficacy. *Cancer Biol. Ther.* **7**, 1952–1958
32. Yang, M., and Vousden, K. H. (2016) Serine and one-carbon metabolism in cancer. *Nat. Rev. Cancer* **16**, 650–662
33. Gu, X., Orozco, J. M., Saxton, R. A., Condon, K. J., Liu, G. Y., Krawczyk, P. A., et al. (2017) SAMTOR is an S-adenosylmethionine sensor for the mTORC1 pathway. *Science* **358**, 813–818
34. Sakata, S. F., Okumura, S., Matsuda, K., Horikawa, Y., Maeda, M., Kawasaki, K., et al. (2005) Effect of fasting on methionine adenosyltransferase expression and the methionine cycle in the mouse liver. *J. Nutr. Sci. Vitaminol.* **51**, 118–123
35. Sakata, S. F., Shelly, L. L., Ruppert, S., Schutz, G., and Chou, J. Y. (1993) Cloning and expression of murine S-adenosylmethionine synthetase. *J. Biol. Chem.* **268**, 13978–13986
36. Halim, A. B., LeGros, L., Chamberlin, M. E., Geller, A., and Kotb, M. (2001) Regulation of the human MAT2A gene encoding the catalytic alpha 2 subunit of methionine adenosyltransferase, MAT II: gene organization, promoter characterization, and identification of a site in the proximal promoter that is essential for its activity. *J. Biol. Chem.* **276**, 9784–9791
37. Kotb, M., Mudd, S. H., Mato, J. M., Geller, A. M., Kredich, N. M., Chou, J. Y., et al. (1997) Consensus nomenclature for the mammalian methionine adenosyltransferase genes and gene products. *Trends Genet.* **13**, 51–52
38. LeGros, L., Halim, A. B., Chamberlin, M. E., Geller, A., and Kotb, M. (2001) Regulation of the human MAT2B gene encoding the regulatory beta subunit of methionine adenosyltransferase, MAT II. *J. Biol. Chem.* **276**, 24918–24924
39. Murray, B., Antonyuk, S. V., Marina, A., Van Liempd, S. M., Lu, S. C., Mato, J. M., et al. (2014) Structure and function study of the complex that synthesizes S-adenosylmethionine. *IUCr* **1**, 240–249
40. Bailey, J., Douglas, H., Masino, L., de Carvalho, L. P. S., and Argyrou, A. (2021) Human Mat2A uses an ordered kinetic mechanism and is stabilized but not regulated by Mat2B. *Biochemistry* **60**, 3621–3632
41. Cai, J., Sun, W. M., Hwang, J. J., Stain, S. C., and Lu, S. C. (1996) Changes in S-adenosylmethionine synthetase in human liver cancer: molecular characterization and significance. *Hepatology* **24**, 1090–1097
42. Huang, Z.-Z., Mao, Z., Cai, J., and Lu, S. C. (1998) Changes in methionine adenosyltransferase during liver regeneration in the rat. *Am. J. Physiol. Gastrointest. Liver Physiol.* **275**, G14–G21
43. Frau, M., Feo, F., and Pascale, R. M. (2013) Pleiotropic effects of methionine adenosyltransferases deregulation as determinants of liver cancer progression and prognosis. *J. Hepatol.* **59**, 830–841
44. Liu, T., Yang, H., Fan, W., Tu, J., Li, T. W. H., Wang, J., et al. (2018) Mechanisms of MAFG dysregulation in cholestatic liver injury and development of liver cancer. *Gastroenterology* **155**, 557–571.e14
45. Chen, H., Gu, B., Zhao, X., Zhao, Y., Huo, S., Liu, X., et al. (2020) Circular RNA hsa\_circ\_0007364 increases cervical cancer progression through activating methionine adenosyltransferase II alpha (MAT2A) expression by restraining microRNA-101-5p. *Bioengineered* **11**, 1269–1279
46. Tomasi, M. L., Ryoo, M., Skay, A., Tomasi, I., Giordano, P., Mato, J. M., et al. (2013) Polyamine and methionine adenosyltransferase 2A crosstalk in human colon and liver cancer. *Exp. Cell Res.* **319**, 1902–1911
47. Phuong, N. T. T., Kim, S. K., Im, J. H., Yang, J. W., Choi, M. C., Lim, S. C., et al. (2016) Induction of methionine adenosyltransferase 2A in tamoxifen-resistant breast cancer cells. *Oncotarget* **7**, 13902–13916
48. Villa, E., Sahu, U., O'Hara, B. P., Ali, E. S., Helmin, K. A., Asara, J. M., et al. (2021) mTORC1 stimulates cell growth through SAM synthesis and m6A mRNA-dependent control of protein synthesis. *Mol. Cell* **81**, 2076–2093.e9
49. Polevoda, B., and Sherman, F. (2007) Methylation of proteins involved in translation. *Mol. Microbiol.* **65**, 590–606
50. Malecki, J., Aileni, V. K., Ho, A. Y. Y., Schwarz, J., Moen, A., Sørensen, V., et al. (2017) The novel lysine specific methyltransferase METTL21B affects mRNA translation through inducible and dynamic methylation of Lys-165 in human eukaryotic elongation factor 1 alpha (eEF1A). *Nucleic Acids Res.* **45**, 4370–4389
51. Liu, S., Hausmann, S., Carlson, S. M., Fuentes, M. E., Francis, J. W., Pillai, R., et al. (2019) METTL13 methylation of eEF1A increases translational output to promote tumorigenesis. *Cell* **176**, 491–504.e21
52. Schmidt, E. K., Clavarino, G., Ceppi, M., and Pierre, P. (2009) SUnSET, a nonradioactive method to monitor protein synthesis. *Nat. Methods* **6**, 275–277
53. Jani, T. S., Gobejishvili, L., Hote, P. T., Barve, A. S., Joshi-Barve, S., Kharebava, G., et al. (2009) Inhibition of methionine adenosyltransferase II induces FasL expression, Fas-DISC formation and caspase-8-dependent apoptotic death in T leukemic cells. *Cell Res.* **19**, 358–369
54. Sufrin, J. R., Coulter, A. W., and Talalay, P. (1979) Structural and conformational analogues of L-methionine as inhibitors of the enzymatic synthesis of S-adenosyl-L-methionine. IV. Further mono-, bi- and tricyclic amino acids. *Mol. Pharmacol.* **15**, 661–677
55. Gingras, A. C., Raught, B., and Sonenberg, N. (1999) eIF4 initiation factors: effectors of mRNA recruitment to ribosomes and regulators of translation. *Annu. Rev. Biochem.* **68**, 913–963
56. Monaco, P. L., Marcel, V., Diaz, J.-J., and Catez, F. (2018) 2'-O-Methylation of ribosomal RNA: towards an epitranscriptomic control of translation? *Biomolecules* **8**, E106
57. Henras, A. K., Plisson-Chastang, C., O'Donohue, M.-F., Chakraborty, A., and Gleizes, P.-E. (2015) An overview of pre-ribosomal RNA processing in eukaryotes. *Wiley Interdiscip. Rev. RNA* **6**, 225–242
58. Zhao, S., Chen, Y., Chen, F., Huang, D., Shi, H., Lo, L. J., et al. (2019) Sas10 controls ribosome biogenesis by stabilizing Mpp10 and delivering the Mpp10–Imp3–Imp4 complex to nucleolus. *Nucleic Acids Res.* **47**, 2996–3012
59. Corsini, N. S., Peer, A. M., Moeseneder, P., Roiuk, M., Burkard, T. R., Theussl, H.-C., et al. (2018) Coordinated control of mRNA and rRNA processing controls embryonic stem cell pluripotency and differentiation. *Cell Stem Cell* **22**, 543–558.e12
60. Figaro, S., Wacheul, L., Schillewaert, S., Graille, M., Huvelle, E., Mongeard, R., et al. (2012) Trm112 is required for Bud23-mediated

- methylation of the 18S rRNA at position G1575. *Mol. Cell. Biol.* **32**, 2254–2267
61. Ishiguro, K., Arai, T., and Suzuki, T. (2019) Depletion of S-adenosylmethionine impacts on ribosome biogenesis through hypomodification of a single rRNA methylation. *Nucleic Acids Res.* **47**, 4226–4239
  62. Shubina, M. Y., Musinova, Y. R., and Sheval, E. V. (2016) Nucleolar methyltransferase fibrillarlin: evolution of structure and functions. *Biochemistry (Mosc.)* **81**, 941–950
  63. Hamey, J. J., and Wilkins, M. R. (2018) Methylation of elongation factor 1A: where, who, and why? *Trends Biochem. Sci.* **43**, 211–223
  64. Li, Z., Gonzalez, P. A., Sasvari, Z., Kinzy, T. G., and Nagy, P. D. (2014) Methylation of translation elongation factor 1A by the METTL10-like See1 methyltransferase facilitates tombusvirus replication in yeast and plants. *Virology* **448**, 43–54
  65. Swiercz, R., Person, M. D., and Bedford, M. T. (2005) Ribosomal protein S2 is a substrate for mammalian PRMT3 (protein arginine methyltransferase 3). *Biochem. J.* **386**, 85–91
  66. White, J. T., Cato, T., Deramchi, N., Gabunilas, J., Roy, K. R., Wang, C., et al. (2019) Protein methylation and translation: role of lysine modification on the function of yeast elongation factor 1A. *Biochemistry* **58**, 4997–5010
  67. Davydova, E., Ho, A. Y. Y., Malecki, J., Moen, A., Enserink, J. M., Jakobsson, M. E., et al. (2014) Identification and characterization of a novel evolutionarily conserved lysine-specific methyltransferase targeting eukaryotic translation elongation factor 2 (eEF2). *J. Biol. Chem.* **289**, 30499–30510
  68. Ong, S.-E., Mittler, G., and Mann, M. (2004) Identifying and quantifying *in vivo* methylation sites by heavy methyl SILAC. *Nat. Methods* **1**, 119–126
  69. Newbery, H. J., Loh, D. H., O'Donoghue, J. E., Tomlinson, V. A. L., Chau, Y.-Y., Boyd, J. A., et al. (2007) Translation elongation factor eEF1A2 is essential for post-weaning survival in mice. *J. Biol. Chem.* **282**, 28951–28959
  70. Hoffman, R. M. (1982) Methionine dependence in cancer cells - a review. *In Vitro* **18**, 421–428
  71. Mecham, J. O., Rowitch, D., Wallace, C. D., Stern, P. H., and Hoffman, R. M. (1983) The metabolic defect of methionine dependence occurs frequently in human tumor cell lines. *Biochem. Biophys. Res. Commun.* **117**, 429–434
  72. Módis, K., Coletta, C., Asimakopoulou, A., Szczesny, B., Chao, C., Papapetropoulos, A., et al. (2014) Effect of S-adenosyl-L-methionine (SAM), an allosteric activator of cystathionine- $\beta$ -synthase (CBS) on colorectal cancer cell proliferation and bioenergetics *in vitro*. *Nitric Oxide* **41**, 146–156
  73. Obata, F., Tsuda-Sakurai, K., Yamazaki, T., Nishio, R., Nishimura, K., Kimura, M., et al. (2018) Nutritional control of stem cell division through S-adenosylmethionine in *Drosophila* intestine. *Dev. Cell* **44**, 741–751.e3
  74. Saito, Y., Iwatsuki, K., Hanyu, H., Maruyama, N., Aihara, E., Tadaishi, M., et al. (2017) Effect of essential amino acids on enteroids: methionine deprivation suppresses proliferation and affects differentiation in enteroid stem cells. *Biochem. Biophys. Res. Commun.* **488**, 171–176
  75. Shiraki, N., Shiraki, Y., Tsuyama, T., Obata, F., Miura, M., Nagae, G., et al. (2014) Methionine metabolism regulates maintenance and differentiation of human pluripotent stem cells. *Cell Metab.* **19**, 780–794
  76. Booher, K., Lin, D.-W., Borrego, S. L., and Kaiser, P. (2012) Down-regulation of Cdc6 and pre-replication complexes in response to methionine stress in breast cancer cells. *Cell Cycle* **11**, 4414–4423
  77. Lu, S., and Epner, D. E. (2000) Molecular mechanisms of cell cycle block by methionine restriction in human prostate cancer cells. *Nutr. Cancer* **38**, 123–130
  78. Shima, H., Matsumoto, M., Ishigami, Y., Ebina, M., Muto, A., Sato, Y., et al. (2017) S-adenosylmethionine synthesis is regulated by selective N6-adenosine methylation and mRNA degradation involving METTL16 and YTHDC1. *Cell Rep.* **21**, 3354–3363
  79. Li, T. W. H., Yang, H., Peng, H., Xia, M., Mato, J. M., and Lu, S. C. (2012) Effects of S-adenosylmethionine and methylthioadenosine on inflammation-induced colon cancer in mice. *Carcinogenesis* **33**, 427–435
  80. Zsigrai, S., Kalmár, A., Nagy, Z. B., Barták, B. K., Valcz, G., Szigeti, K. A., et al. (2020) S-adenosylmethionine treatment of colorectal cancer cell lines alters DNA methylation, DNA repair and tumor progression-related gene expression. *Cells* **9**, E1864
  81. Cave, D. D., Desiderio, V., Mosca, L., Ilisso, C. P., Mele, L., Caraglia, M., et al. (2018) S-Adenosylmethionine-mediated apoptosis is potentiated by autophagy inhibition induced by chloroquine in human breast cancer cells. *J. Cell Physiol.* **233**, 1370–1383
  82. Yan, L., Liang, X., Huang, H., Zhang, G., Liu, T., Zhang, J., et al. (2019) S-adenosylmethionine affects cell cycle pathways and suppresses proliferation in liver cells. *J. Cancer* **10**, 4368–4379
  83. Sancak, Y., Peterson, T. R., Shaul, Y. D., Lindquist, R. A., Thoreen, C. C., Bar-Peled, L., et al. (2008) The Rag GTPases bind raptor and mediate amino acid signaling to mTORC1. *Science* **320**, 1496–1501
  84. Caboche, M., and Bachellerie, J. P. (1977) RNA methylation and control of eukaryotic RNA biosynthesis. Effects of cycloleucine, a specific inhibitor of methylation, on ribosomal RNA maturation. *Eur. J. Biochem.* **74**, 19–29
  85. Morello, L. G., Coltri, P. P., Quaresma, A. J. C., Simabuco, F. M., Silva, T. C. L., Singh, G., et al. (2011) The human nucleolar protein FTSJ3 associates with NIP7 and functions in pre-rRNA processing. *PLoS One* **6**, e29174
  86. Yi, Y., Li, Y., Meng, Q., Li, Q., Li, F., Lu, B., et al. (2021) A PRC2-independent function for EZH2 in regulating rRNA 2'-O methylation and IRES-dependent translation. *Nat. Cell Biol.* **23**, 341–354
  87. Katoh, Y., Ikura, T., Hoshikawa, Y., Tashiro, S., Ito, T., Ohta, M., et al. (2011) Methionine adenosyltransferase II serves as a transcriptional corepressor of Maf oncoprotein. *Mol. Cell* **41**, 554–566
  88. Kera, Y., Katoh, Y., Ohta, M., Matsumoto, M., Takano-Yamamoto, T., and Igarashi, K. (2013) Methionine adenosyltransferase II-dependent histone H3K9 methylation at the COX-2 gene locus. *J. Biol. Chem.* **288**, 13592–13601
  89. Xiao, S., Wang, Y., Ma, Y., Liu, J., Tang, C., Deng, A., et al. (2020) Dimethylation of eEF1A at lysine 55 plays a key role in the regulation of eEF1A2 on malignant cell functions of acute myeloid leukemia. *Technol. Cancer Res. Treat.* **19**, 1533033820914295
  90. Jakobsson, M. E., Malecki, J. M., Halabelian, L., Nilges, B. S., Pinto, R., Kudithipudi, S., et al. (2018) The dual methyltransferase METTL13 targets N terminus and Lys55 of eEF1A and modulates codon-specific translation rates. *Nat. Commun.* **9**, 3411
  91. Hua, X., Ge, S., Chen, J., Zhang, L., Tai, S., and Liang, C. (2020) Effects of RNA binding proteins on the prognosis and malignant progression in prostate cancer. *Front. Genet.* **11**, 591667
  92. Wu, Y.-Q., Ju, C.-L., Wang, B.-J., and Wang, R.-G. (2019) PABPC1L depletion inhibits proliferation and migration via blockage of AKT pathway in human colorectal cancer cells. *Oncol. Lett.* **17**, 3439–3445
  93. Rikova, K., Hall, B., Levy, T., Possemato, A., Wang, Y., Lee, K., et al. (2013) Abstract B197: proteomic based analysis of ovarian cancer pathways. *Mol. Cancer Ther.* **12**, B197
  94. Wu, Z., Cheng, Z., Sun, M., Wan, X., Liu, P., He, T., et al. (2015) A chemical proteomics approach for global analysis of lysine monomethylome profiling. *Mol. Cell. Proteomics* **14**, 329–339
  95. Derry, M. C., Yanagiya, A., Martineau, Y., and Sonenberg, N. (2006) Regulation of poly(A)-binding protein through PABP-interacting proteins. *Cold Spring Harb. Symp. Quant. Biol.* **71**, 537–543
  96. Gray, N. K., Coller, J. M., Dickson, K. S., and Wickens, M. (2000) Multiple portions of poly(A)-binding protein stimulate translation *in vivo*. *EMBO J.* **19**, 4723–4733
  97. Jackson, R. J., Hellen, C. U. T., and Pestova, T. V. (2010) The mechanism of eukaryotic translation initiation and principles of its regulation. *Nat. Rev. Mol. Cell Biol.* **11**, 113–127
  98. Endres, L., Rose, R. E., Doyle, F., Rahn, T., Lee, B., Seaman, J., et al. (2020) 2'-O-ribose methylation of transfer RNA promotes recovery from oxidative stress in *Saccharomyces cerevisiae*. *PLoS One* **15**, e0229103

## mTORC1-independent translation control by MAT2A and SAM

99. Liu, F., Clark, W., Luo, G., Wang, X., Fu, Y., Wei, J., *et al.* (2016) ALKBH1-mediated tRNA demethylation regulates translation. *Cell* **167**, 816–828.e16
100. Tuorto, F., Liebers, R., Musch, T., Schaefer, M., Hofmann, S., Kellner, S., *et al.* (2012) RNA cytosine methylation by Dnmt2 and NSun2 promotes tRNA stability and protein synthesis. *Nat. Struct. Mol. Biol.* **19**, 900–905
101. Dumont, F. J., Staruch, M. J., Grammer, T., Blenis, J., Kastner, C. A., and Rupperecht, K. M. (1995) Dominant mutations confer resistance to the immunosuppressant, rapamycin, in variants of a T cell lymphoma. *Cell Immunol.* **163**, 70–79
102. Lorenz, M. C., and Heitman, J. (1995) TOR mutations confer rapamycin resistance by preventing interaction with FKBP12-rapamycin. *J. Biol. Chem.* **270**, 27531–27537
103. Sarbassov, D. D., Guertin, D. A., Ali, S. M., and Sabatini, D. M. (2005) Phosphorylation and regulation of Akt/PKB by the rictor-mTOR complex. *Science* **307**, 1098–1101
104. Tamburini, J., Chapuis, N., Bardet, V., Park, S., Sujobert, P., Willems, L., *et al.* (2008) Mammalian target of rapamycin (mTOR) inhibition activates phosphatidylinositol 3-kinase/Akt by up-regulating insulin-like growth factor-1 receptor signaling in acute myeloid leukemia: rationale for therapeutic inhibition of both pathways. *Blood* **111**, 379–382
105. Dilling, M. B., Germain, G. S., Dudkin, L., Jayaraman, A. L., Zhang, X., Harwood, F. C., *et al.* (2002) 4E-binding proteins, the suppressors of eukaryotic initiation factor 4E, are down-regulated in cells with acquired or intrinsic resistance to rapamycin. *J. Biol. Chem.* **277**, 13907–13917
106. Kaplan, B., Qazi, Y., and Wellen, J. R. (2014) Strategies for the management of adverse events associated with mTOR inhibitors. *Transplant. Rev. (Orlando)* **28**, 126–133
107. de Boer, E., Rodriguez, P., Bonte, E., Krijgsveld, J., Katsantoni, E., Heck, A., *et al.* (2003) Efficient biotinylation and single-step purification of tagged transcription factors in mammalian cells and transgenic mice. *Proc. Natl. Acad. Sci. U. S. A.* **100**, 7480–7485
108. Matsuo, Y., Ikeuchi, K., Saeki, Y., Iwasaki, S., Schmidt, C., Udagawa, T., *et al.* (2017) Ubiquitination of stalled ribosome triggers ribosome-associated quality control. *Nat. Commun.* **8**, 159
109. Ochiai, K., Shima, H., Ikura, T., Franke, M. C., Sievert, E. P., Sciammas, R., *et al.* (2021) Protocol for *in vitro* BCR-mediated plasma cell differentiation and purification of chromatin-associated proteins. *STAR Protoc.* **2**, 100633
110. Tanaka, H., Muto, A., Shima, H., Katoh, Y., Sax, N., Tajima, S., *et al.* (2016) Epigenetic regulation of the Blimp-1 gene (Prdm1) in B cells involves Bach2 and histone deacetylase 3. *J. Biol. Chem.* **291**, 6316–6330
111. Yasuda, S., Tsuchiya, H., Kaiho, A., Guo, Q., Ikeuchi, K., Endo, A., *et al.* (2020) Stress- and ubiquitylation-dependent phase separation of the proteasome. *Nature* **578**, 296–300
112. Cao, X.-J., Zee, B. M., and Garcia, B. A. (2013) Heavy methyl-SILAC labeling coupled with liquid chromatography and high-resolution mass spectrometry to study the dynamics of site-specific histone methylation. *Methods Mol. Biol.* **977**, 299–313
113. Musiani, D., Bok, J., Massignani, E., Wu, L., Tabaglio, T., Ippolito, M. R., *et al.* (2019) Proteomics profiling of arginine methylation defines PRMT5 substrate specificity. *Sci. Signal.* **12**, eaat8388
114. Frazier, M. L., Mars, W., Florine, D. L., Montagna, R. A., and Saunders, G. F. (1983) Efficient extraction of RNA from mammalian tissue. *Mol. Cell. Biochem.* **56**, 113–122